Table 4 Univariate analysis of pretreatment factors associated with interferon-induced neutropenia

	Case-G2 + R[a] ($n = 100$)	Control-G + R[b] ($n = 656$)	P value[c]
Gender, male/female	45/55	378/278	0.018
Age, years	58.1 (9.3)	56.9 (10.4)	0.262
Neutrophil count, /mm^3	1,614 (735)	2,742 (979)	<0.001
Hemoglobin, g/dL	13.5 (1.5)	14.2 (1.5)	<0.001
Platelet count, $\times 10^9$/L	136 (46)	163 (57)	<0.001
ALT, IU/L	79.1 (69.7)	83.5 (74.3)	0.574
HCV RNA, log IU/ml	6.0 (0.9)	6.1 (0.8)	0.164
Liver fibrosis, F0-2/F3-4/ND	46/16/38	397/157/102	0.674
rs2305482, AA + AC/CC/ND	74/24/2	591/59/6	<0.001
rs4794822, TT + TC/CC/ND	56/42/2	484/130/42	<0.001

Data are expressed as number for categorical data or the mean (standard deviation) for non-categorical data

ALT alanine transaminase, *ND* not determined

[a] Case-G2 + R: Case-G2 plus Case-R

[b] Control-G + R: Control-G plus Control-R

[c] Categorical variables were compared between groups by the Chi square test and non-categorical variables by the Student's t test

Table 5 Logistic regression analysis of pretreatment factors associated with interferon-induced neutropenia

	OR (95 % CI)	P value
Gender, female	1.229 (0.734–2.059)	0.4331
Neutrophil count, /mm^3	0.998 (0.997–0.998)	<0.0001
Platelet count, $\times 10^9$/L	1.005 (0.953–1.059)	0.8604
rs2305482, CC	2.497 (1.281–4.864)	0.0072

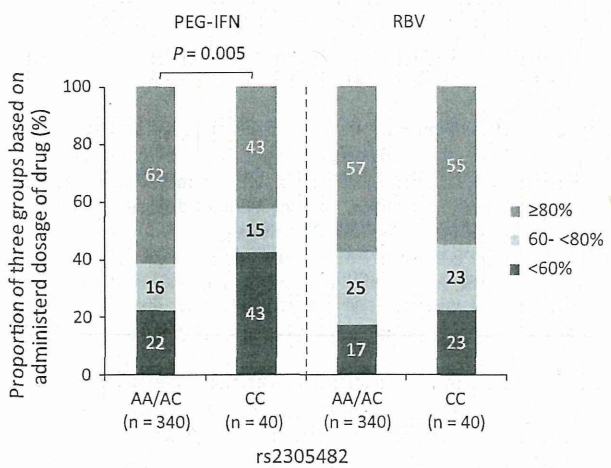

Fig. 3 Administered doses of PEG-IFN and RBV according to rs2305482 genotypes. The patients were stratified into three groups according to the doses of PEG-IFN or RBV administered, as follows: <60 %, ≥60 to <80 %, ≥80 % of the planned doses for 48 weeks. The proportion of patients receiving <60 % of the PEG-IFN doses was significantly higher in patients with rs2305482 CC than in those with AA/AC ($P = 0.005$, by the Chi square test). *PEG-IFN* pegylated interferon, *RBV* ribavirin

reasons for the dose reduction of PEG-IFN in PEG-IFN/RBV therapy. While, there were no associations between SVR and rs2305482 or rs4794822 genotypes (Supplementary Table 3).

PSMD3 encodes the proteasome 26S subunit, non-ATPase 3, a member of the 26S proteasome family, and is involved in the control of cell cycle transition via the ubiquitin–proteasome pathway (Bailly and Reed 1999). *CSF3* encodes G-CSF, which controls the production, differentiation, and function of granulocytes (Nagata et al. 1986). Recombinant G-CSF is widely used to treat patients with severe neutropenia during chemotherapy. Therefore, we hypothesize that *PSMD3-CSF3* variants may influence neutrophil counts through affecting the process of endogenous G-CSF synthesis during IFN-based therapy or other bone marrow suppressive therapies. However, eQTL analysis by Okada et al. (2010) showed that rs4794822 was significantly associated with the expression level of *PSMD3*, rather than that of *CSF3* in the JPT and CHB populations. Our eQTL analysis showed that the risk allele for neutropenia at rs2305482 correlated with higher expression levels of *PSMD3* in LWK and MEX populations (Supplementary Fig. 5a), whereas with lower expression levels of *CSF3* in MEX and especially in CHB populations (Supplementary Fig. 5b, c). However, these results were not replicated in the other probe of *CSF3*. Additionally, we analyzed serum G-CSF levels in CHC patients receiving IFN-based therapy. Although serum G-CSF levels were thought to be increased in response to neutropenia regardless of rs2305482 and rs4794822 genotypes, there was no evidence that they were lower in patients with a risk allele of these SNPs at baseline and during the neutropenic period (Supplementary Fig. 6). Moreover, neutrophil counts did not correlate with serum

G-CSF levels at baseline and the time of minimum neutrophil counts (Supplementary Fig. 7a). Further functional analyses of these genes and polymorphisms are required to elucidate the reason for the association between *PSMD3-CSF3* and IFN-induced neutropenia as well as neutrophil counts in healthy individuals.

In previous reports, *PLBC4*, *DARC*, *CXCL2*, and *CDK5* loci have also been associated with neutrophil or WBC counts in healthy individuals or patients who were not under chemotherapy (Crosslin et al. 2012; Kamatani et al. 2010; Okada et al. 2010; Reiner et al. 2011). However, there were no associations with these loci discernible in our GWAS.

The important limitation of this study is that the association between rs2305482 and IFN-induced neutropenia was not statistically significant in a genome-wide level. Thompson et al. (2012) also identified no genetic determinants of IFN-induced neutropenia during PEG-IFN/RBV therapy at the level of genome-wide significance by their GWAS. Unlike our study design, they analyzed the association between the reduction of neutrophil counts at week 4 and any SNPs. Indeed, we analyzed the association between the reduction of neutrophil counts at week 2 or 4 and rs2305482 or rs4794822, but there was no significant association. Therefore, further independent replication analyses which are designed in the similar way as our study are desirable.

IFN-free therapies are expected to be useful especially in IFN-resistant patients and may become the standard of care in the near future. However, combination therapies of DAA and IFN will continue to be used for some time. Our findings contribute to our understanding of the genetic factors influencing IFN-induced neutropenia. Furthermore, these genetic variants may be associated with neutropenia during chemotherapies for various malignant diseases as well as IFN-based therapy for CHC. Therefore, genetic testing of these variants might be useful for establishing personalized doses of such therapies to minimize drug-induced adverse events. Additionally, our results might contribute to the elucidation of the mechanism of drug-induced neutropenia.

Acknowledgments We thank Ms. Yasuka Uehara-Shibata, Yuko Ogasawara-Hirano, Yoshimi Ishibashi, Natsumi Baba, Megumi Yamaoka-Sageshima, Takayo Tsuchiura, Yoriko Mawatari (Tokyo University), and Dr. Shintaro Ogawa (Nagoya City University) for technical assistance. This work was supported by the Ministry of Health, Labor, and Welfare of Japan (H25-kanen-ippan-005) to Yasuhito Tanka and Katsushi Tokunaga, KAKENHI (22133008) Grant-in-Aid for Scientific Research on Innovative Areas to Katsushi Tokunaga, and KAKENHI (24790728) Grant-in-Aid from the Ministry of Education, Culture, Sports, Science of Japan for Young Scientists (B) to Nao Nishida.

Conflict of interest The following authors are currently conducting research sponsored by the companies: Yasuhito Tanaka, Keisuke Hino, and Yoshito Itoh by Merck Sharp & Dohme, Corp., Chugai Pharmaceutical Co., Ltd., and Bristol-Myers Squibb; Nobuyuki Enomoto, Shuhei Nishiguchi, and Eiji Tanaka by Merck Sharp & Dohme, Corp. and Chugai Pharmaceutical Co., Ltd.; Naoya Sakamoto by Chugai Pharmaceutical Co., Ltd, Bristol-Myers Squibb, Merck Sharp & Dohme, Corp., and Otsuka Pharmaceutical Co., Ltd.; Hiroshi Yatsuhashi by Chugai Pharmaceutical Co., Ltd.; Akihiro Tamori by Merck Sharp & Dohme, Corp.; Satoshi Mochida by Merck Sharp & Dohme, Corp., Chugai Pharmaceutical Co., Ltd., Bristol-Myers Squibb, and Toray Medical Co., Ltd. The other authors have no conflict of interest.

Compliance with ethical standards All procedures performed in studies involving human participants were in accordance with the ethical standards of the institutional and/or national research committee and with the 1964 Helsinki declaration and its later amendments or comparable ethical standards. This article does not contain any studies with animals performed by any of the authors.

Informed consent Informed consent was obtained from all individual participants included in the study.

References

Bailly E, Reed SI (1999) Functional characterization of rpn3 uncovers a distinct 19S proteasomal subunit requirement for ubiquitin-dependent proteolysis of cell cycle regulatory proteins in budding yeast. Mol Cell Biol 19:6872–6890

Crosslin DR, McDavid A, Weston N, Nelson SC, Zheng X, Hart E, de Andrade M, Kullo IJ, McCarty CA, Doheny KF, Pugh E, Kho A, Hayes MG, Pretel S, Saip A, Ritchie MD, Crawford DC, Crane PK, Newton K, Li R, Mirel DB, Crenshaw A, Larson EB, Carlson CS, Jarvik GP (2012) Genetic variants associated with the white blood cell count in 13,923 subjects in the eMERGE Network. Hum Genet 131:639–652. doi:10.1007/s00439-011-1103-9

Fellay J, Thompson AJ, Ge D, Gumbs CE, Urban TJ, Shianna KV, Little LD, Qiu P, Bertelsen AH, Watson M, Warner A, Muir AJ, Brass C, Albrecht J, Sulkowski M, McHutchison JG, Goldstein DB (2010) ITPA gene variants protect against anaemia in patients treated for chronic hepatitis C. Nature 464:405–408. doi:10.1038/nature08825

Ge D, Fellay J, Thompson AJ, Simon JS, Shianna KV, Urban TJ, Heinzen EL, Qiu P, Bertelsen AH, Muir AJ, Sulkowski M, McHutchison JG, Goldstein DB (2009) Genetic variation in IL28B predicts hepatitis C treatment-induced viral clearance. Nature 461:399–401. doi:10.1038/nature08309

George SL, Bacon BR, Brunt EM, Mihindukulasuriya KL, Hoffmann J, Di Bisceglie AM (2009) Clinical, virologic, histologic, and biochemical outcomes after successful HCV therapy: a 5-year follow-up of 150 patients. Hepatology 49:729–738. doi:10.1002/hep.22694

Jacobson IM, McHutchison JG, Dusheiko G, Di Bisceglie AM, Reddy KR, Bzowej NH, Marcellin P, Muir AJ, Ferenci P, Flisiak R, George J, Rizzetto M, Shouval D, Sola R, Terg RA, Yoshida EM, Adda N, Bengtsson L, Sankoh AJ, Kieffer TL, George S, Kauffman RS, Zeuzem S (2011) Telaprevir for previously untreated chronic hepatitis C virus infection. N Engl J Med 364:2405–2416. doi:10.1056/NEJMoa1012912

Kamatani Y, Matsuda K, Okada Y, Kubo M, Hosono N, Daigo Y, Nakamura Y, Kamatani N (2010) Genome-wide association study of hematological and biochemical traits in a Japanese population. Nat Genet 42:210–215. doi:10.1038/ng.531

Kurosaki M, Tanaka Y, Tanaka K, Suzuki Y, Hoshioka Y, Tamaki N, Kato T, Yasui Y, Hosokawa T, Ueda K, Tsuchiya K, Kuzuya T,

Nakanishi H, Itakura J, Takahashi Y, Asahina Y, Matsuura K, Sugauchi F, Enomoto N, Nishida N, Tokunaga K, Mizokami M, Izumi N (2011) Relationship between polymorphisms of the inosine triphosphatase gene and anaemia or outcome after treatment with pegylated interferon and ribavirin. Antivir Ther 16:685–694. doi:10.3851/IMP1796

Matsuura K, Tanaka Y, Watanabe T, Fujiwara K, Orito E, Kurosaki M, Izumi N, Sakamoto N, Enomoto N, Yatsuhashi H, Kusakabe A, Shinkai N, Nojiri S, Joh T, Mizokami M (2014) ITPA genetic variants influence efficacy of PEG-IFN/RBV therapy in older patients infected with HCV genotype 1 and favourable IL28B type. J Viral Hepat 21:466–474. doi:10.1111/jvh.12171

McHutchison JG, Manns M, Patel K, Poynard T, Lindsay KL, Trepo C, Dienstag J, Lee WM, Mak C, Garaud JJ, Albrecht JK (2002) Adherence to combination therapy enhances sustained response in genotype-1-infected patients with chronic hepatitis C. Gastroenterology 123:1061–1069

Nagata S, Tsuchiya M, Asano S, Kaziro Y, Yamazaki T, Yamamoto O, Hirata Y, Kubota N, Oheda M, Nomura H et al (1986) Molecular cloning and expression of cDNA for human granulocyte colony-stimulating factor. Nature 319:415–418. doi:10.1038/319415a0

Nishida N, Tanabe T, Takasu M, Suyama A, Tokunaga K (2007) Further development of multiplex single nucleotide polymorphism typing method, the DigiTag2 assay. Anal Biochem 364:78–85. doi:10.1016/j.ab.2007.02.005

Ochi H, Maekawa T, Abe H, Hayashida Y, Nakano R, Kubo M, Tsunoda T, Hayes CN, Kumada H, Nakamura Y, Chayama K (2010) ITPA polymorphism affects ribavirin-induced anemia and outcomes of therapy—a genome-wide study of Japanese HCV virus patients. Gastroenterology 139:1190–1197. doi:10.1053/j.gastro.2010.06.071

Okada Y, Kamatani Y, Takahashi A, Matsuda K, Hosono N, Ohmiya H, Daigo Y, Yamamoto K, Kubo M, Nakamura Y, Kamatani N (2010) Common variations in PSMD3-CSF3 and PLCB4 are associated with neutrophil count. Hum Mol Genet 19:2079–2085. doi:10.1093/hmg/ddq080

Poordad F, Bronowicki JP, Gordon SC, Zeuzem S, Jacobson IM, Sulkowski MS, Poynard T, Morgan TR, Molony C, Pedicone LD, Sings HL, Burroughs MH, Sniukiene V, Boparai N, Goteti VS, Brass CA, Albrecht JK, Bacon BR (2012) Factors that predict response of patients with hepatitis C virus infection to boceprevir. Gastroenterology 143(608–18):e1–e5. doi:10.1053/j.gastro.2012.05.011

Reiner AP, Lettre G, Nalls MA, Ganesh SK, Mathias R, Austin MA, Dean E, Arepalli S, Britton A, Chen Z, Couper D, Curb JD, Eaton CB, Fornage M, Grant SF, Harris TB, Hernandez D, Kamatini N, Keating BJ, Kubo M, LaCroix A, Lange LA, Liu S, Lohman K, Meng Y, Mohler ER 3rd, Musani S, Nakamura Y, O'Donnell CJ, Okada Y, Palmer CD, Papanicolaou GJ, Patel KV, Singleton AB, Takahashi A, Tang H, Taylor HA Jr, Taylor K, Thomson C, Yanek LR, Yang L, Ziv E, Zonderman AB, Folsom AR, Evans MK, Liu Y, Becker DM, Snively BM, Wilson JG (2011) Genome-wide association study of white blood cell count in 16,388 African Americans: the continental origins and genetic epidemiology network (COGENT). PLoS Genet 7:e1002108. doi:10.1371/journal.pgen.1002108

Sakamoto N, Tanaka Y, Nakagawa M, Yatsuhashi H, Nishiguchi S, Enomoto N, Azuma S, Nishimura-Sakurai Y, Kakinuma S, Nishida N, Tokunaga K, Honda M, Ito K, Mizokami M, Watanabe M (2010) ITPA gene variant protects against anemia induced by pegylated interferon-alpha and ribavirin therapy for Japanese patients with chronic hepatitis C. Hepatol Res 40:1063–1071. doi:10.1111/j.1872-034X.2010.00741.x

Soranzo N, Spector TD, Mangino M, Kuhnel B, Rendon A, Teumer A, Willenborg C, Wright B, Chen L, Li M, Salo P, Voight BF, Burns P, Laskowski RA, Xue Y, Menzel S, Altshuler D, Bradley JR, Bumpstead S, Burnett MS, Devaney J, Doring A, Elosua R, Epstein SE, Erber W, Falchi M, Garner SF, Ghori MJ, Goodall AH, Gwilliam R, Hakonarson HH, Hall AS, Hammond N, Hengstenberg C, Illig T, Konig IR, Knouff CW, McPherson R, Melander O, Mooser V, Nauck M, Nieminen MS, O'Donnell CJ, Peltonen L, Potter SC, Prokisch H, Rader DJ, Rice CM, Roberts R, Salomaa V, Sambrook J, Schreiber S, Schunkert H, Schwartz SM, Serbanovic-Canic J, Sinisalo J, Siscovick DS, Stark K, Surakka I, Stephens J, Thompson JR, Volker U, Volzke H, Watkins NA, Wells GA, Wichmann HE, Van Heel DA, Tyler-Smith C, Thein SL, Kathiresan S, Perola M, Reilly MP, Stewart AF, Erdmann J, Samani NJ, Meisinger C, Greinacher A, Deloukas P, Ouwehand WH, Gieger C (2009) A genome-wide meta-analysis identifies 22 loci associated with eight hematological parameters in the HaemGen consortium. Nat Genet 41:1182–1190. doi:10.1038/ng.467

Suppiah V, Moldovan M, Ahlenstiel G, Berg T, Weltman M, Abate ML, Bassendine M, Spengler U, Dore GJ, Powell E, Riordan S, Sheridan D, Smedile A, Fragomeli V, Muller T, Bahlo M, Stewart GJ, Booth DR, George J (2009) IL28B is associated with response to chronic hepatitis C interferon-alpha and ribavirin therapy. Nat Genet 41:1100–1104. doi:10.1038/ng.447

Tanaka Y, Nishida N, Sugiyama M, Kurosaki M, Matsuura K, Sakamoto N, Nakagawa M, Korenaga M, Hino K, Hige S, Ito Y, Mita E, Tanaka E, Mochida S, Murawaki Y, Honda M, Sakai A, Hiasa Y, Nishiguchi S, Koike A, Sakaida I, Imamura M, Ito K, Yano K, Masaki N, Sugauchi F, Izumi N, Tokunaga K, Mizokami M (2009) Genome-wide association of IL28B with response to pegylated interferon-alpha and ribavirin therapy for chronic hepatitis C. Nat Genet 41:1105–1109. doi:10.1038/ng.449

Tanaka Y, Kurosaki M, Nishida N, Sugiyama M, Matsuura K, Sakamoto N, Enomoto N, Yatsuhashi H, Nishiguchi S, Hino K, Hige S, Itoh Y, Tanaka E, Mochida S, Honda M, Hiasa Y, Koike A, Sugauchi F, Kaneko S, Izumi N, Tokunaga K, Mizokami M (2011) Genome-wide association study identified ITPA/DDRGK1 variants reflecting thrombocytopenia in pegylated interferon and ribavirin therapy for chronic hepatitis C. Hum Mol Genet 20:3507–3516. doi:10.1093/hmg/ddr249

Thompson AJ, Clark PJ, Singh A, Ge D, Fellay J, Zhu M, Zhu Q, Urban TJ, Patel K, Tillmann HL, Naggie S, Afdhal NH, Jacobson IM, Esteban R, Poordad F, Lawitz EJ, McCone J, Shiffman ML, Galler GW, King JW, Kwo PY, Shianna KV, Noviello S, Pedicone LD, Brass CA, Albrecht JK, Sulkowski MS, Goldstein DB, McHutchison JG, Muir AJ (2012) Genome-wide association study of interferon-related cytopenia in chronic hepatitis C patients. J Hepatol 56:313–319. doi:10.1016/j.jhep.2011.04.021

Yang TP, Beazley C, Montgomery SB, Dimas AS, Gutierrez-Arcelus M, Stranger BE, Deloukas P, Dermitzakis ET (2010) Genevar: a database and Java application for the analysis and visualization of SNP-gene associations in eQTL studies. Bioinformatics 26:2474–2476. doi:10.1093/bioinformatics/btq452

Yoshida H, Tateishi R, Arakawa Y, Sata M, Fujiyama S, Nishiguchi S, Ishibashi H, Yamada G, Yokosuka O, Shiratori Y, Omata M (2004) Benefit of interferon therapy in hepatocellular carcinoma prevention for individual patients with chronic hepatitis C. Gut 53:425–430

Zeuzem S, Andreone P, Pol S, Lawitz E, Diago M, Roberts S, Focaccia R, Younossi Z, Foster GR, Horban A, Ferenci P, Nevens F, Mullhaupt B, Pockros P, Terg R, Shouval D, van Hoek B, Weiland O, Van Heeswijk R, De Meyer S, Luo D, Boogaerts G, Polo R, Picchio G, Beumont M (2011) Telaprevir for retreatment of HCV infection. N Engl J Med 364:2417–2428. doi:10.1056/NEJMoa1013086

J Gastroenterol (2015) 50:203–210
DOI 10.1007/s00535-014-0954-y

The Japanese Society of Gastroenterology

ORIGINAL ARTICLE—LIVER, PANCREAS, AND BILIARY TRACT

CTNNB1 mutational analysis of solid-pseudopapillary neoplasms of the pancreas using endoscopic ultrasound-guided fine-needle aspiration and next-generation deep sequencing

Yoshimasa Kubota · Hiroshi Kawakami · Mitsuteru Natsuizaka · Kazumichi Kawakubo · Katsuji Marukawa · Taiki Kudo · Yoko Abe · Kimitoshi Kubo · Masaki Kuwatani · Yutaka Hatanaka · Tomoko Mitsuhashi · Yoshihiro Matsuno · Naoya Sakamoto

Received: 30 January 2014 / Accepted: 19 March 2014 / Published online: 4 April 2014

Abstract
Background Solid-pseudopapillary neoplasm (SPN), a rare neoplasm of the pancreas, frequently harbors mutations in exon 3 of the cadherin-associated protein beta 1 (*CTNNB1*) gene. Here, we analyzed SPN tissue for *CTNNB1* mutations by deep sequencing using next-generation sequencing (NGS).
Methods Tissue samples from 7 SPNs and 31 other pancreatic lesions (16 pancreatic ductal adenocarcinomas (PDAC), 11 pancreatic neuroendocrine tumors (PNET), 1 acinar cell carcinoma, 1 autoimmune pancreatitis lesion, and 2 focal pancreatitis lesions) were analyzed by NGS for mutations in exon 3 of *CTNNB1*.
Results A single-base-pair missense mutations in exon 3 of *CTNNB1* was observed in all 7 SPNs and in 1 of 11 PNET samples. However, mutations were not observed in the tissue samples of any of the 16 PDAC or other four pancreatic disease cases. The variant frequency of *CTNNB1* ranged from 5.4 to 48.8 %.
Conclusions Mutational analysis of *CTNNB1* by NGS is feasible and was achieved using SPN samples obtained by endoscopic ultrasound-guided fine needle aspiration.

Y. Kubota · H. Kawakami (✉) · M. Natsuizaka · K. Kawakubo · T. Kudo · Y. Abe · K. Kubo · M. Kuwatani · N. Sakamoto
Department of Gastroenterology and Hepatology, Hokkaido University Graduate School of Medicine, Kita-15, Nishi-7, Kita-ku, Sapporo 060-8638, Japan
e-mail: hiropon@med.hokudai.ac.jp

K. Marukawa · Y. Hatanaka · T. Mitsuhashi · Y. Matsuno
Department of Surgical Pathology, Hokkaido University Hospital, Sapporo, Japan

Keywords *CTNNB1* · Solid-pseudopapillary neoplasms of the pancreas · Endoscopic ultrasound-guided fine-needle aspiration (EUS-FNA) · Next-generation sequencing

Introduction

Solid-pseudopapillary neoplasm (SPN) of the pancreas is a rare tumor that accounts for 0.2–2.7 % of all pancreatic tumors [1], predominantly seen in young female patients. It was first described by Frantz [2] in 1959. SPN of the pancreas is characterized by low-grade malignant potential, with an incidence of metastasis of 15 %, and tends to have a favorable prognosis with surgical resections, considered the standard of care, with a 5-year overall survival rate of more than 95 % [1, 3, 4].

β-Catenin is a submembranous component of the cadherin-mediated cell adhesion system and acts as a downstream transcriptional activator of Wnt signaling. Under normal conditions, cytoplasmic β-catenin is expressed at a low level. Phosphorylation of both adenomatous polyposis coli (APC) and axin by glycogen synthase kinase-3β (GSK-3β) enhances β-catenin binding to the APC-axin complex and targets the protein for ubiquitination and proteasomal degradation [5]. In the nucleus, β-catenin forms complexes with proteins such as Tcf and Lef-1 [6], and activates the transcription of several oncogenic genes including c-myc and cyclin D1.

Mutations in exon 3 of the β-catenin gene (also called *CTNNB1*) are reported in approximately 83–100 % [7–12] of surgically resected SPN samples. Accordingly, these mutations are considered a unique genetic characteristic of SPNs, differentiating them from other pancreatic tumors.

Direct sequencing is considered the gold standard for mutational analysis. However, it is difficult to detect a

small proportion of mutant genes using this method. Recently, next-generation sequencing (NGS) has enabled the evaluation of multiple genes for genomic alterations in a single tumor, with high accuracy [13]. Less frequent mutations can also be detected if deep sequencing is performed.

Several studies have described the usefulness of EUS-guided fine-needle aspiration (EUS-FNA) for diagnosing SPNs [14–18]. SPNs could be seen as well-demarcated, hypoechoic, solid masses that sometimes coexist with cystic lesions and/or calcification on EUS. Accuracy of preoperative SPN diagnosis by EUS-FNA is reported to be 75–100 % [17, 18]; however, diagnosis by EUS-FNA is sometimes difficult because of interpretative, sampling, and misclassification errors or insufficient material for immunostaining [19]. In addition, EUS-FNA samples sometimes contain tumor cells that are too small to use for sequencing analysis by polymerase chain reaction (PCR)-based direct sequencing.

In the present study, we analyzed *CTNNB1* mutations using EUS-FNA samples and NGS. To the best of our knowledge, this is the first report of *CTNNB1* mutational analysis using EUS-FNA samples and NGS.

Methods

Samples

Thirty-eight samples were tested: 7 SPNs, 16 pancreatic ductal adenocarcinomas (PDAC), 11 pancreatic neuroendocrine tumors (PNET), and 4 other pancreatic lesions. Non-SPN samples were used as controls. Samples were obtained by either EUS-FNA ($n = 35$) or surgery ($n = 3$) at Hokkaido University Hospital, Sapporo, Japan, between December 2008 and June 2013. All participants provided written informed consent, and the ethics committee at Hokkaido University Graduate School of Medicine approved the study.

EUS-FNA procedure

EUS-FNA was performed by a single experienced endoscopist (H.K.) using a curvilinear echoendoscope (GF-UCT240-AL5; Olympus Medical Systems Co., Tokyo, Japan) and 22-gauge needles (Echotip Ultra; Cook Japan, Tokyo, Japan) with the patient under conscious sedation. Briefly, the lesions were visualized by EUS, and the needle was advanced into the lesion through the gastric or duodenal wall. The central stylet was removed, and a syringe was attached to the needle hub to apply negative suction pressure. The needle was then moved back and forth within the lesion at least 10 times and then removed through the scope, before the stylet was re-inserted into the needle. The specimen obtained by aspiration was placed on a slide, air-dried, alcohol-fixed, and used to prepare smears that were stained using the rapid Romanowsky technique for quick interpretation and assessment of sample adequacy (Diff-Quik stain; Kokusai Shiyaku, Kobe, Japan). Diff-Quik staining was performed on all specimens by an experienced cytotechnologist (K.M.). Cytological and histological diagnoses were made for the specimens obtained by EUS-FNA [20, 21].

DNA extraction, PCR, and sequencing analysis of *CTNNB1*

The FNA samples were stored in RNAlater (Life Technologies Corporation, Carlsbad, CA). Genomic DNA and RNA were extracted from samples using an AllPrep® DNA/RNA/Protein mini kit (Qiagen, Inc., Valencia, CA) according to the manufacturer's instructions. Three PNET samples were obtained from surgery. Tumor samples were fixed in 10 % buffered formalin and embedded in paraffin for microdissection of the tumor tissue. Genomic DNA was semi-automatically extracted using a QIAamp® DNA FFPE tissue kit (Qiagen) and QIAcube® (Qiagen) according to the manufacturer's instructions. Total RNA concentration was determined by spectrophotometer (NanoDrop2000/2000c; Thermo Scientific, Tokyo, Japan), and 5 μg total RNA were reverse transcribed using SuperScript® II Reverse Transcriptase (Invitrogen, Carlsbad, CA). Approximately 100 ng of each genomic DNA sample were used for PCR. Genomic DNA was amplified by semi-nested PCR, using the first and second primer pairs (Table 1). Primers for the second PCR contained adaptors and barcodes for further NGS analysis, and the PCR products were bidirectionally read by NGS. These primers were designed to amplify a 228-bp DNA fragment of the entire exon 3 of *CTNNB1*. The thermal cycler (Life Technologies) was programmed as follows: initial denaturation at 94 °C for 7 min and 35 amplification cycles for each PCR. Each amplification cycle comprised denaturation at 94 °C for 15 s, annealing at 58 °C for 15 s, and elongation at 72 °C for 30 s. The last cycle was followed by a final extension at 72 °C for 5 min. The PCR products were verified by agarose gel electrophoresis. The band of the expected size was excised and purified using a QIAquick® Gel Extraction kit (Qiagen).

The concentration and amplicon size of the barcoded libraries were determined by using an Agilent 2100 Bioanalyzer and Agilent DNA 1000 kit (Agilent Technologies, Inc., Santa Clara, CA).

They were pooled and mixed with Ion Spheres™ particles for emulsion PCR using the Ion OneTouch™ System (Life Technologies) with an Ion OneTouch™

Table 1 Primers used in this study

Primers for the first PCR
Forward
5′-CTGATTTGATGGAGTTGGACATGG-3′
Reverse
5′-CAGCTACTTGTTCTTGAGTGAAGG-3′
Primers for the second PCR (library preparation for next-generation sequencing)
Primer pair for forward sequencing
Forward
5′-CCATCTCATCCCTGCGTGTCTCCGACTCAG-barcode-CTGATTTGATGGAGTTGGACATGG-3′
Reverse
5′-CCTCTCTATGGGCAGTCGGTGATCAGCTACTTGTTCTTGAGTGAAGG-3′
Primer pair for reverse sequencing
Forward
5′-CCATCTCATCCCTGCGTGTCTCCGACTCAG-barcode-CAGCTACTTGTTCTTGAGTGAAGG-3′
Reverse
5′-CCTCTCTATGGGCAGTCGGTGATCTGATTTGATGGAGTTGGACATGG-3′

Template kit v2 (Life Technologies) according to the manufacturer's instructions. Samples were subsequently enriched using Ion OneTouch™ ES (Life Technologies). The final concentration of the template for emulsion PCR was 0.4 pM. Sequencing was performed on an Ion PGM™ (Personal Genome Machine) Sequencer by using an Ion 314™ chip (Life Technologies) with an Ion-PGM™ Sequencing 200 kit (Life Technologies) according to the manufacturer's protocol. Obtained sequences were mapped onto the human reference genome hg19, and variants were detected using Ion Torrent Suite v2.2 software (Life Technologies).

The PCR products were also submitted to direct sequencing using ABI Big Dye Terminator v1.1 Cycle Sequencing Kit (Applied Biosystems, Foster City, CA) and the primers used for PCR. Sequencing of each PCR product was performed with an ABI PRISM™ 310 Genetic Analyzer (Applied Biosystems). Each mutation was verified in both sense and antisense directions.

Results

Clinicopathological features

The clinicopathological features of the 38 patients are summarized in Table 2. The patient population comprised 24 women and 14 men, with ages ranging from 13 to 81 years (median 63.5 years). SPNs tended to be located in the pancreatic body and tail rather than in the pancreatic head. Other tumors involved all parts of the pancreas and were evenly distributed. Tumor sizes ranged from 8 to 95 mm at the greatest diameter (median 23 mm).

The types of surgical procedures were as follows: three subtotal stomach-preserving pancreaticoduodenectomies, two duodenum-preserving pancreas head resections, seven distal pancreatectomies (four with splenectomy and one with spleen and left adrenal gland resection), one partial pancreatectomy, and one left nephrectomy with metastatic lymph node tumor resection. Two patients with PDAC had resectable disease, whereas the other cases were unresectable.

The histological features of the specimens with SPN obtained by EUS-FNA are shown in Fig. 1. In most cases, SPN showed typical findings, but in case 7, SPN was not easily distinguished from PNET. Immunohistochemical staining was performed for SPN and PNET samples. Two SPNs showed a few chromogranin A-positive cells, five of seven SPNs showed immunoreactivity against Synaptophysin, and five SPNs showed nuclear staining for β-catenin. All PNET samples were positive for chromogranin A and synaptophysin, and none showed nuclear immunoreactivity against β-catenin.

Genomic DNA and RNA were extracted from FNA samples in 35 patients. For three PNET patients (Case 24, 25 and 26), surgically resected specimens were used to obtain DNA.

Mutations in exon 3 of *CTNNB1* by NGS

All seven SPNs showed a single-base-pair missense mutation in exon 3 of *CTNNB1*. Neither the PDAC nor acinar cell carcinoma cases showed a *CTNNB1* exon 3 mutation. Of the 11 PNETs, a single-base-pair missense mutation was detected in one sample. Variant frequency and coverage ranged from 5.4 to 48.8 % and from 4,490 to

Table 2 Clinicopathological features

Case	Final diagnosis	Sex	Age	Location in pancreas	Tumor size (mm)	Radiological feature	Tumor markers		Procedure for the final diagnosis	Surgical procedure	Results of immunohistochemical staining		
							CEA (ng/mL)	CA19-9 (IU/mL)			CgA	Synaptophysin	β-Catenin
1	SPN	F	33	Pt	64	Solid/cystic	2	0	Surgery	DP	(−)	(+)	Nuclear
2	SPN	F	31	Pb	12	Solid/cystic	1	6	Surgery	Partial pancreatectomy	(−)	(−)	Nuclear
3	SPN	F	17	Ph	23	Solid/cystic	1	<1	Surgery	DpPHR	(−)	(+)	ND
4	SPN	F	36	Pbt	28	Solid/cystic	2	12	Surgery	DP	(−)	(+)	Nuclear
5	SPN	F	27	Pt	48	Solid/cystic	1	<1	Surgery	DP	(+)	(+)	Nuclear
6	SPN	F	13	Ph	63	Solid/cystic	1	9	Surgery	DpPHR	(+)	(+)	Nuclear
7	SPN	F	26	Pb	13	Solid	1	8	EUS-FNA	ND	(−)	(−)	ND
8	PDAC	F	64	Ph	33	Solid	10	3	Surgery	SSPPD	ND	ND	ND
9	PDAC	F	75	Pt	22	Solid	55	220	Surgery	DP	ND	ND	ND
10	PDAC	F	55	Ph	45	Solid	12	693	EUS-FNA	ND	ND	ND	ND
11	PDAC	M	62	Pt	70	Solid	79	>10,000	EUS-FNA	ND	ND	ND	ND
12	PDAC	F	76	Ph	70	Solid/cystic	4	>10,000	EUS-FNA	ND	ND	ND	ND
13	PDAC	M	64	Ph	17	Solid	22	53	EUS-FNA	ND	ND	ND	ND
14	PDAC	F	81	Ph	9	Solid	2	21	EUS-FNA	ND	ND	ND	ND
15	PDAC	F	78	Pt	66	Solid	12	361	EUS-FNA	ND	ND	ND	ND
16	PDAC	F	67	Ph	10	Solid	7	242	EUS-FNA	ND	ND	ND	ND
17	PDAC	M	63	Ph	27	Solid	7	2,320	EUS-FNA	ND	ND	ND	ND
18	PDAC	M	57	Ph	17	Solid	6	30	EUS-FNA	ND	ND	ND	ND
19	PDAC	M	79	Ph	30	Solid	3	871	EUS-FNA	ND	ND	ND	ND
20	PDAC	M	44	Pbt	28	Solid	48	2,880	EUS-FNA	ND	ND	ND	ND
21	PDAC	M	78	Pt	27	Solid	3	229	EUS-FNA	ND	ND	ND	ND
22	PDAC	F	67	Ph	25	Solid	15	246	EUS-FNA	ND	ND	ND	ND
23	PDAC	M	80	Pt	47	Solid	440	>10,000	EUS-FNA	ND	ND	ND	ND
24	PNET	F	58	Pt	23	Solid	2	14	Surgery	DP	(+)	(+)	ND
25	PNET	M	51	Ph	52	Solid/cystic	2	31	Surgery	SSPPD	(+)	(+)	ND
26[a]	PNET	F	76	Lymph node	18	Solid	3	11	Surgery	Left nephrectomy	(+)	(+)	ND
27[b]	PNET	M	72	Pt	20	Solid	5	14	Surgery	DP	(+)	(+)	ND
28	PNET	F	58	Pb	18	Solid	2	14	Surgery	DP	(+)	(+)	ND
29	PNET	F	78	Ph	16	Solid	2	<1	Surgery	SSPPD	(+)	(+)	ND
30	PNET	M	79	Pb	9	Solid	3	8	EUS-FNA	ND	(+)	(+)	Membrane
31	PNET	F	69	Pt	8	Solid	3	5	EUS-FNA	ND	(+)	(+)	ND
32	PNET	F	77	Ph	17	Solid	2	47	EUS-FNA	ND	(+)	(+)	ND
33	PNET	F	45	Ph	17	Solid/cystic	3	26	EUS-FNA	ND	(+)	(+)	ND

Table 2 continued

Case	Final diagnosis	Sex	Age	Location in pancreas	Tumor size (mm)	Radiological feature	Tumor markers		Procedure for the final diagnosis	Surgical procedure	Results of immunohistochemical staining		
							CEA (ng/mL)	CA19-9 (IU/mL)			CgA	Synaptophysin	β-Catenin
34	PNET	F	62	Ph	10	Solid/cystic	6	40	EUS-FNA	ND	(+)	(+)	ND
35	Acinar cell carcinoma	M	46	Pbt	95	Solid/cystic	4	19	EUS-FNA	ND	(+)	(−)	ND
36	AIP	M	72	Pt	28	Solid	8	22	EUS-FNA	ND	ND	ND	ND
37	Focal pancreatitis	F	42	Pt	20	Solid/cystic	1	6	EUS-FNA	ND	ND	ND	ND
38	Focal pancreatitis	M	64	Ph	22	Solid	4	<1	EUS-FNA	ND	ND	ND	ND

SPN solid-pseudopapillary neoplasm, *PDAC* pancreatic ductal adenocarcinoma, *PNET* pancreatic neuroendocrine tumor, *AIP* autoimmune pancreatitis, *M* male, *F* female, *Ph* pancreatic head, *Pb* pancreatic body, *Pt* pancreatic tail, *CEA* carcinoembryonic antigen, *CA19-9* carbohydrate antigen 19-9, *EUS-FNA* endoscopic ultrasound-guided fine-needle aspiration, *DP* distal pancreatectomy, *DpPHR* duodenum-preserving pancreas head resection, *SSPPD* subtotal stomach-preserving pancreaticoduodenectomy, *CgA* chromogranin A, *ND* not done

[a] The patient of case 26 developed a metastatic lymph node tumor 5 years after the initial surgery for PNET. Secondary surgery was a left nephrectomy with metastatic lymph node tumor resection

[b] The patient of case 27 had mixed ductal-neuroendocrine carcinoma and two synchronous PNETs

203,919, respectively. For the sample with a variant frequency of 5.39, the read depth was 15,199. The involved codons were as follows: codon 32 (three cases), codon 37 (two cases), and codon 41 (three cases). The results of the analysis are shown in Table 3. For the control samples, the average base coverage depth ranged from 113 to 8,027 (median 7,312).

Mutations in exon 3 of *CTNNB1* by direct sequencing

Direct sequencing was performed using samples that had mutations detected by NGS. One SPN case with mutation was not able to perform direct sequencing due to an insufficient amount of the sample. Only one of the seven cases could detect mutation by direct sequencing, as shown also in Table 3.

Discussion

Mutations in exon 3 of *CTNNB1* have been reported in various tumors, including those of the colon [22], prostate [23], endometrium [24], and liver [25].

In SPN, cytoplasmic/nuclear immunoreactivity for β-catenin was detected during the systemic immunohistochemical study of pediatric tumors [7]. After the first report by Tanaka et al. [7], mutations in exon 3 of *CTNNB1* have been reported in 83–100 % [7–12] of SPNs. Previous studies used microdissected tumor tissue from formalin-fixed, paraffin-embedded blocks obtained by surgery to extract genomic DNA. Single-base-pair missense mutations in codons 32, 33, 34, 37, and 41, and 12-base-pair deletion corresponding to codons 28–32 have been documented.

Serine 33 and 37 as well as threonine 41 are the sites for GSK-3 β phosphorylation [26]. Codons 32 and 34 serve as crucial elements of the DSGΦXS motif to create a recognition site for β-TrCP and subsequent ubiquitin-mediated proteasomal degradation [27, 28]. Both mechanisms lead to the abnormal stabilization of β-catenin and its resultant aberrant nuclear expression in SPNs.

In the present study, eight cases showed *CTNNB1* mutations. Mutations were detected in codons 32, 37, and 41, consistent with the findings of previous reports [7–12]. To the best of our knowledge, this is the first report of mutational analysis for *CTNNB1* using EUS-FNA samples and NGS. Of the eight cases, seven were of SPN and one was of PNET. That PNET was diagnosed by the typical radiologic finding (a hypervascular round mass that was best visualized in the arterial contrast enhancement phase on computed tomography) and immunohistochemical staining (positive chromogranin A and synaptophysin immunostaining, negative CD56 staining, and no nuclear

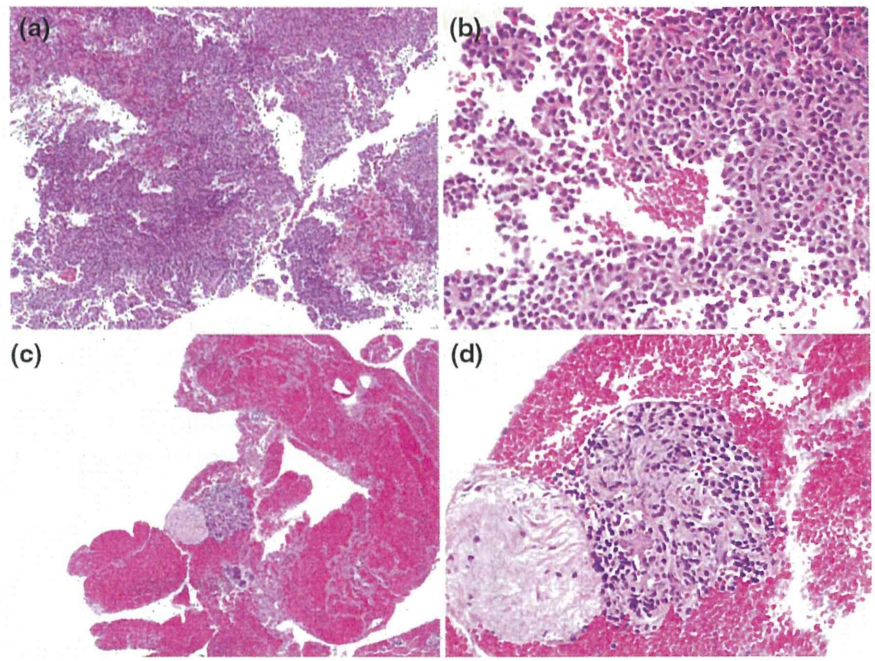

Fig. 1 Histological features of solid-pseudopapillary neoplasm specimens obtained by endoscopic ultrasonography-guided fine-needle aspiration. **a**, **b** Typical specimen (case 4). Small and uniform neoplastic cells have either eosinophilic or clear vacuolated cytoplasm. These loosely cohesive cells surround the delicate vessels and form pseudopapillae. **c**, **d** Atypical specimen (case 7). The specimen contains a small number of neoplastic cells in the fibrous stroma that do not form apparent pseudopapillae. The small and uniform neoplastic cells have eosinophilic cytoplasm and show a plasmacytoid appearance. These clusters are difficult to distinguish from those of neuroendocrine tumors

Table 3 Mutations in *CTTNB1*

Case	Template	Mutated codon	Nucleotide	AA substitution	Var. freq (%)	Coverage	Ref cov.	Var cov.	Direct seq
1	RNA	37	N378 C/A	Ser37Tyr	23.81	19,047	14,495	4,535	Undetectable
2	RNA	32	N363 A/G	Asp32Gly	5.39	16,072	15,199	866	Undetectable
3	RNA	32	N362 G/C	Asp32His	48.77	25,740	13,161	12,554	Undetectable
4	gDNA	41	N390 C/T	Thr41Ile	31.07	4,490	3,093	1,395	Undetectable
5	gDNA	37	N378 C/T	Ser37Phe	26.48	115,799	84,609	30,665	Detectable
6	gDNA	41	N362 G/A	Asp32Asn	21.50	203,919	43,842	160,077	Undetectable
7	RNA	41	N390 C/T	Thr41Ile	29.68	35,808	25,167	10,629	NA

AA amino acid, *Var Freq* variant frequency, *Ref Cov* reference coverage, *Var Cov* variantcoverage, *Direct seq* direct sequencing, *gDNA* genomic DNA, *Ser* serine, *Tyr* tyrosine,*Asp* asparatic acid, *Gly* glycine, *His* histidine, *Thr* threonine, *Ile* isoleucine, *Phe*phenylalanine, *Asn* asparagine, *NA* not available

β-catenin accumulation) of an EUS-FNA sample. The patient did not undergo surgery because of the small size (9.6 × 5.4 mm) and low-grade malignant potential of the lesion, which was diagnosed on the basis of EUS-FNA specimen analysis (Ki-67 index, 1–2 %).

Several assays can be performed to detect genetic mutations, such as hematoxylin and eosin and immunohistochemical staining, fluorescence in-situ hybridization, polymerase chain reaction, and direct sequencing. Although direct sequencing is considered the gold standard, it lacks the ability to detect small proportions of mutant genes and technical experience is essential for accurate result interpretation. In one study, mutant DNA had to account for at least 30 % of wild-type DNA for the detection of mutations by direct sequencing [29]. In our study, mutations caught by NGS could be detected in only one of seven samples by direct sequencing. Our result showed the superiority of NGS in detecting mutations over direct sequencing, as indicated in previous reports. This result suggests the usefulness of FNA specimens for genetic analyses when combined with NGS, since EUS-FNA specimens are usually mixed with blood or tissue in the needle tract.

To date, *CTNNB1* mutations have not been reported in PNET. Gerdes et al. [30] previously performed *CTNNB1* mutational analysis on 78 PDAC, 33 PNET, and 14 pancreatic cancer cell lines and found no mutations in exon 3 of *CTNNB1*. Similarly, Liu et al. [10] found no mutations in exon 3 of *CTNNB1* in 14 PNET samples. Exome sequence analysis of approximately 18,000 protein-coding

genes of 10 PNET samples was carried out by Jiao et al. [31] to explore the genetic basis of the disease. They reported novel *DAXX* and *ATRX* mutations, but mutations in *CTNNB1* were not detected. With regard to neuroendocrine tumors in other organs, Kim et al. [32] detected a single-base-pair mutation in one of two thymus neuroendocrine tumors, which resulted in a replacement of isoleucine by serine at codon 35. Another mutation was seen in a cell line of neuroendocrine tumor of midgut (terminal ileum) origin [33]. To explore whether *CTNNB1* mutations occur in PNET, we enrolled two more cases of PNET that were diagnosed by surgery, but did not detect any mutations. Further analysis should be performed to determine if *CTNNB1* mutations occur in PNET.

One of the most important differential diagnoses of SPN is PNET [16, 34]. Histologically, most SPNs show a solidmonomorphous growth in the peripheral parts of the lesion. In the center, tumor cells form pseudopapillary structures [35]. PNETs are morphologically very similar to SPNs. Immunostaining is useful in differentiating SPNs from PNETs. SPNs specifically express vimentin and CD10 [8, 36] and usually show focal immunoreactivity against synaptophysin, but not for chromogranin A. On the other hand, PNETs usually show diffuse staining for synaptophysin. Strong staining for chromogranin A is observed in differentiated neuroendocrine tumors, NETs, but negative or very mild staining is found in poorly differentiated lesions [37, 38]. β-Catenin localization is also quite different between these two tumor types. SPNs show cytoplasmic and nuclear staining [3, 7], but PNETs show membranous staining. Accurate diagnosis of SPNs is sometimes difficult with EUS-FNA because of interpretative, sampling, and misclassification errors or insufficient material for immunostaining [19]. In the present study, 1 case of SPN could not be diagnosed pathologically on the basis of EUS-FNA samples. However, the *CTNNB1* mutation was detected by NGS, and the patient was diagnosed as having SPN and was scheduled for surgery at the time of reporting.

The current study was limited by two points. First, not all of the mutational analyses were performed prior to the final diagnosis by either EUS-FNA or surgery. Second, being a rare tumor, the sample size was rather small.

Conclusions

Analysis of exon 3 mutations in *CTNNB1* by NGS is feasible using EUS-FNA samples. All SPN cases showed *CTNNB1* mutations. Further exploration of mutational analyses including *CTNNB1* in neuroendocrine tumors is required to determine the genetic alterations of PNET.

Conflict of interest The authors declare that they have no conflict of interest.

References

1. Papavramidis T, Papavramidis S. Solid pseudopapillary tumors of the pancreas: review of 718 patients reported in English literature. J Am Coll Surg. 2005;200:965–72.
2. Frantz VK. Tumors of the pancreas. Atlas of tumor pathology, 1st series. Washington DC: Armed Forces Institute of Pathology; 1959.
3. Klimstra DS, Wenig BM, Heffess CS. Solid-pseudopapillary tumor of the pancreas: a typically cystic carcinoma of low malignant potential. Semin Diagn Pathol. 2000;17:66–80.
4. Yu PF, Hu ZH, Wang XB, et al. Solid pseudopapillary tumor of the pancreas: a review of 553 cases in Chinese literature. World J Gastroenterol. 2010;16:1209–14.
5. Behrens J, Jerchow BA, Würtele M, et al. Functional interaction of an axin homolog, conductin, with beta-catenin, APC, and GSK3beta. Science. 1998;280:596–9.
6. Aoki M, Hecht A, Kruse U, et al. Nuclear endpoint of Wnt signaling: neoplastic transformation induced by transactivating lymphoid-enhancing factor 1. Proc Natl Acad Sci USA. 1999;96:139–44.
7. Tanaka Y, Kato K, Notohara K, et al. Frequent ß-catenin mutation and cytoplasmic/nuclear accumulation in pancreatic solid-pseudopapillary neoplasm. Cancer Res. 2001;61:8401–4.
8. Abraham SC, Klimstra DS, Wilentz RE, et al. Solid-pseudopapillary tumors of the pancreas are genetically distinct from pancreatic ductal adenocarcinomas and almost always harbor beta-catenin mutations. Am J Pathol. 2002;160:1361–9.
9. Takahashi Y, Hiraoka N, Onozato K, et al. Solid-pseudopapillary neoplasms of the pancreas in men and women: do they differ? Virchows Arch. 2006;448:561–9.
10. Liu BA, Li ZM, Su ZS, et al. Pathological differential diagnosis of solid-pseudopapillary neoplasm and endocrine tumors of the pancreas. World J Gastroenterol. 2010;16:1025–30.
11. Wu J, Jiao Y, Dal Molin M, et al. Whole-exome sequencing of neoplastic cysts of the pancreas reveals recurrent mutations in components of ubiquitin-dependent pathways. Proc Natl Acad Sci USA. 2011;108:21188–93.
12. Huang SC, Ng KF, Yeh TS, et al. Clinicopathological analysis of beta-catenin and axin-1 in solid pseudopapillary neoplasms of the pancreas. Ann Surg Oncol. 2011;19(Suppl 3):S438–46.
13. Ross JS, Ali SM, Wang K, et al. Comprehensive genomic profiling of epithelial ovarian cancer by next generation sequencing-based diagnostic assay reveals new routes to targeted therapies. Gynecol Oncol. 2013;130:554–9.
14. Nadler EP, Novikov A, Landzberg BR, et al. The use of endoscopic ultrasound in the diagnosis of solid pseudopapillary tumor of the pancreas in children. J Pediatr Surg. 2002;37:1370–3.
15. Master SS, Savides T. Diagnosis of solid pseudopapillary neoplasm of the pancreas by EUS-guided FNA. Gastrointest Endosc. 2003;57:965–9.
16. Bardales RH, Centeno B, Mallery JS, et al. Endoscopic ultrasound-guided fine-needle aspiration cytology diagnosis of solid pseudopapillary tumor of the pancreas: a rare neoplasm of elusive origin but characteristic cytomorphologic features. Am J Clin Pathol. 2004;121:654–62.
17. Jani N, Dewitt J, Eloubeidi M, et al. Endoscopic ultrasound-guided fine-needle aspiration for diagnosis of solid pseudopapillary tumors of pancreas: a multicenter experience. Endoscopy. 2008;40:200–3.

18. Maimone A, Luigiano C, Baccarini P, et al. Preoperative diagnosis of a solid pseudopapillary tumour of the pancreas by endoscopic ultrasound fine needle biopsy: a retrospective case series. Dig Liver Dis. 2013;45:957–60.
19. Hooper K, Mukhtar F, Li S, et al. Diagnostic error assessment and associated harm of endoscopic ultrasound-guided fine-needle aspiration of neuroendocrine neoplasms of the pancreas. Cancer Cytopathol. 2013. doi:10.1002/cncy.21332).
20. Haba S, Yamao K, Bhatia V, et al. Diagnostic ability and factors affecting accuracy of endoscopic ultrasound-guided fine needle aspiration for pancreatic solid lesions: Japanese large single center experience. J Gastroenterol. 2013;48:973–81.
21. Eto K, Kawakami H, Kuwatani M, et al. Human equilibrative nucleoside transporter 1 and Notch3 can predict gemcitabine effects in patients with unresectable pancreatic cancer. Br J Cancer. 2013;108:1488–94.
22. Morin PJ, Sparks AB, Korinek V, et al. Activation of ß-catenin-Tcf signaling in colon cancer by mutations in ß-catenin or APC. Science. 1997;275:1787–90.
23. Voeller HJ, Truica CI, Gelmann EP. ß-catenin mutations in human prostate cancer. Cancer Res. 1998;58:2520–3.
24. Palacios J, Gamallo C. Mutations in the ß-catenin gene (CTNNB1) in endometrioid ovarian carcinomas. Cancer Res. 1998;58:1344–7.
25. Miyoshi Y, Iwao K, Nagasawa Y, et al. Activation of the ß-catenin gene in primary hepatocellular carcinomas by somatic alterations involving exon 3. Cancer Res. 1998;58:2524–7.
26. Liu C, Li Y, Semenov M, et al. Control of beta-catenin phosphorylation/degradation by a dual-kinase mechanism. Cell. 2002;108:837–47.
27. Wu R, Zhai Y, Fearon ER, et al. Diverse mechanisms of beta-catenin deregulation in ovarian endometrioid adenocarcinomas. Cancer Res. 2001;61:8247–55.
28. Wu G, Xu G, Schulman BA, et al. Structure of a beta-TrCP-1-Skp1-beta-catenin complex: destruction motif binding and lysine specificity of the SCF (beta-TrCP1) ubiquitin ligase. Mol Cell. 2003;11:1445–56.
29. Angulo B, Conde E, Suárez-Gauthier A, et al. A comparison of EGFR mutation testing methods in lung carcinoma: direct sequencing, real-time PCR and immunohistochemistry. PLoS One. 2012;7:e43842.
30. Gerdes B, Ramaswamy A, Simon B, et al. Analysis of beta-catenin gene mutations in pancreatic tumors. Digestion. 1999;60:544–8.
31. Jiao Y, Shi C, Edil BH, et al. DAXX/ATRX, MEN1, and mTOR pathway genes are frequently altered in pancreatic neuroendocrine tumors. Science. 2011;331:1199–203.
32. Kim JT, Li J, Jang ER, et al. Deregulation of Wnt/β-catenin signaling through genetic or epigenetic alterations in human neuroendocrine tumors. Carcinogenesis. 2013;34:953–61.
33. Rinner B, Gallè B, Trajanoski S, et al. Molecular evidence for the bi-clonal origin of neuroendocrine tumor derived metastases. BMC Genom. 2012;13:594–602.
34. Vassos N, Agaimy A, Klein P, et al. Solid-pseudopapillary neoplasm (SPN) of the pancreas: case series and literature review on an enigmatic entity. Int J Clin Exp Pathol. 2013;6:1051–9.
35. Adamthwaite JA, Verbeke CS, Stringer MD, et al. Solid pseudopapillary tumour of the pancreas: diverse presentation, outcome and histology. JOP. 2006;7:635–42.
36. Notohara K, Hamazaki S, Tsukayama C, et al. Solid pseudopapillary tumor of the pancreas, immunohistochemical localization of neuroendocrine markers and CD10. Am J Surg Pathol. 2000;24:1361–71.
37. Klöppel G, Rindi G, Anlauf M, et al. Site-specific biology and pathology of gastroenteropancreatic neuroendocrine tumors. Virchows Arch. 2007;451:S9–27.
38. Klöppel G, Couvelard A, Perren A, et al. ENETS consensus guidelines for the standards of care in neuroendocrine tumors: towards a standardized approach to the diagnosis of gastroenteropancreatic neuroendocrine tumors and their prognostic stratification. Neuroendocrinology. 2009;90:162–6.

JOURNAL OF VIRAL HEPATITIS
JVH

Journal of Viral Hepatitis, 2014 doi:10.1111/jvh.12312

Sofosbuvir plus ribavirin in Japanese patients with chronic genotype 2 HCV infection: an open-label, phase 3 trial

Masao Omata,[1] Shuhei Nishiguchi,[2] Yoshiyuki Ueno,[3] Hitoshi Mochizuki,[1] Namiki Izumi,[4] Fusao Ikeda,[5] Hidenori Toyoda,[6] Osamu Yokosuka,[7] Kazushige Nirei,[8] Takuya Genda,[9] Takeji Umemura,[10] Tetsuo Takehara,[11] Naoya Sakamoto,[12] Yoichi Nishigaki,[13] Kunio Nakane,[14] Nobuo Toda,[15] Tatsuya Ide,[16] Mikio Yanase,[17] Keisuke Hino,[18] Bing Gao,[19] Kimberly L. Garrison,[19] Hadas Dvory-Sobol,[19] Akinobu Ishizaki,[19] Masa Omote,[19] Diana Brainard,[19] Steven Knox,[19] William T. Symonds,[19] John G. McHutchison,[19] Hiroshi Yatsuhashi[20] and Masashi Mizokami[17] [1]*Yamanashi Prefectural Hospital Organization, Yamanashi, Japan;* [2]*Hyogo College of Medicine, Hyogo, Japan;* [3]*Yamagata University, Yamagata, Japan;* [4]*Musashino Red Cross Hospital, Tokyo, Japan;* [5]*Okayama University, Okayama, Japan;* [6]*Ogaki Municipal Hospital, Gifu, Japan;* [7]*Chiba University, Chiba, Japan;* [8]*Nihon University, Tokyo, Japan;* [9]*Juntendo University, Tokyo, Japan;* [10]*Shinshu University, Nagano, Japan;* [11]*Osaka University, Osaka, Japan;* [12]*Hokkaido University, Hokkaido, Japan;* [13]*Gifu Municipal Hospital, Gifu, Japan;* [14]*Akita City Hospital, Akita, Japan;* [15]*Mitsui Memorial Hospital, Tokyo, Japan;* [16]*Kurume University, Kurume, Japan;* [17]*National Center for Global Health and Medicine, Tokyo, Japan;* [18]*Kawasaki Medical School, Okayama, Japan;* [19]*Gilead Sciences, Inc., Foster City, CA, USA; and* [20]*National Hospital Organization Nagasaki Medical Center, Nagasaki, Japan*

Received June 2014; accepted for publication August 2014

SUMMARY. Genotype 2 hepatitis C virus (HCV) accounts for up to 30% of chronic HCV infections in Japan. The standard of care for patients with genotype 2 HCV – peginterferon and ribavirin for 24 weeks – is poorly tolerated, especially among older patients and those with advanced liver disease. We conducted a phase 3, open-label study to assess the efficacy and safety of an all-oral combination of the NS5B polymerase inhibitor sofosbuvir and ribavirin in patients with chronic genotype 2 HCV infection in Japan. We enrolled 90 treatment-naïve and 63 previously treated patients at 20 sites in Japan. All patients received sofosbuvir 400 mg plus ribavirin (weight-based dosing) for 12 weeks. The primary endpoint was sustained virologic response at 12 weeks after therapy (SVR12). Of the 153 patients enrolled and treated, 60% had HCV genotype 2a, 11% had cirrhosis, and 22% were over the aged 65 or older. Overall, 148 patients (97%) achieved SVR12. Of the 90 treatment-naïve patients, 88 (98%) achieved SVR12, and of the 63 previously treated patients, 60 (95%) achieved SVR12. The rate of SVR12 was 94% in patients with cirrhosis and in those aged 65 and older. No patients discontinued study treatment due to adverse events. The most common adverse events were nasopharyngitis, anaemia and headache. Twelve weeks of sofosbuvir and ribavirin resulted in high rates of SVR12 in treatment-naïve and previously treated patients with chronic genotype 2 HCV infection. The treatment was safe and well tolerated by patients, including the elderly and those with cirrhosis.

Keywords: Hepatitis C virus, HCV genotype 2, direct-acting antiviral agents, nucleotide polymerase inhibitor.

INTRODUCTION

Approximately two million people in Japan – nearly 2% of the population – are chronically infected with the hepatitis C virus (HCV) [1]. The population of patients with chronic HCV infection in Japan differs from that of other countries; patients are generally older, have more advanced liver disease and are more likely to have received previous treatment for HCV infection [2,3]. It is estimated that 15–30% of Japanese patients with HCV will develop serious complications, including liver cirrhosis, end-stage liver disease and hepatocellular carcinoma [4]. Although genotype 1 HCV is currently the most prevalent strain of the virus in Japan, genotype 2 HCV, which now accounts for up to 30% of infections, is rising in prevalence [5]. The current standard of care regimen for the treatment of chronic genotype 2 HCV infection in Japan is 24 weeks of pegylated interferon alpha (Peg-IFNα) and ribavirin (RBV) [6]. Although relatively high rates of SVR

Abbreviations: CI, confidence interval; GCP, Good Clinical Practice; HCV, hepatitis C virus; ICH, International Conference on Harmonization; Peg-IFNα, pegylated interferon alpha; PK, pharmacokinetics; RBV, ribavirin; SVR12, 12 weeks after therapy.

Correspondence: Masao Omata, Yamanashi Prefectural Hospital Organization, 1-1-1 Fujimi, Kofu City, Yamanashi 400-0027, Japan. E-mail: momata-tky@umin.ac.jp

Trial registration details: ClinicalTrials.gov number NCT01910636.

have been reported in clinical trials with this regimen (71–86%), the use of Peg-IFNα+RBV in an ageing population with progressive liver disease is limited by safety and tolerability issues. Moreover, a substantial number of patients have absolute or relative contraindications to interferon. As a result, many Japanese patients with chronic genotype 2 HCV infection have no available treatment options and are thus at risk for worsening of liver disease and complications of cirrhosis, including hepatocellular carcinoma.

Sofosbuvir (Gilead Sciences) is an oral nucleotide analogue inhibitor of the HCV-specific NS5B polymerase that has recently been approved in the United States and Europe for the treatment of chronic HCV infection [7]. The labelled use for patients with chronic genotype 2 HCV infection is sofosbuvir and RBV for 12 weeks. In phase 3 studies, 12 weeks of treatment with sofosbuvir plus RBV in patients infected with genotype 2 HCV resulted in rates of SVR12 of 97% in treatment-naïve patients, 93% in patients ineligible to receive interferon and 86–90% in previously treated patients [8–10].

We conducted a phase 3 trial to determine the efficacy and safety of 12 weeks of sofosbuvir and RBV in treatment-naïve and previously treated Japanese patients with chronic genotype 2 HCV infection with and without compensated cirrhosis.

METHODS

Patients

Patients were enrolled between 16 July 2013 and 30 September 2013 at 20 sites in Japan. Eligible patients were aged 20 years or older with a body weight of at least 40 kg. Patients were required to be chronically infected with genotype 2 HCV and with HCV RNA levels $\geq 10^4$ IU/mL at screening. Planned enrolment was for approximately 84 treatment-naïve and 50 previously treated patients. See Supplement for definitions of types of response to prior treatment.

Up to 40% of enrolled subjects in each group (i.e. treatment naive or treatment experienced) could have evidence of compensated cirrhosis at screening (Child-Pugh A). Cirrhosis was defined as liver biopsy showing a Metavir score of 4 or Ishak score ≥5 or a FibroScan score of >12.5 kPa. Patients were required to have ALT and AST ≤10 × upper limit of the normal range, platelet count ≥50 000 per μL, haemoglobin ≥11 g/dL for women and ≥12 g/dL for men and albumin ≥3 g/dL. There were no upper limits on age or body mass index. Similarly, no restriction was applied to white blood cell or absolute neutrophil count at screening.

Study design

In this multicenter, open-label trial, all patients received 12 weeks of treatment with 400 mg of sofosbuvir, administered orally once daily, and ribavirin (Copegus®, Chugai Pharmaceutical Co., Ltd, Tokyo, Japan), administered orally twice daily, with doses determined according to body weight (600 mg daily in patients with a body weight of ≤60 kg, 800 mg daily in patients weighing >60 and ≤80 kg, and 1000 mg daily in patients with a body weight of >80 kg).

In addition to the main study of efficacy and safety, sparse PK samples were collected from all patients over the course of the study for population PK analyses and all patients were eligible to participate in an optional substudy to determine the steady-state pharmacokinetics (PK) of sofosbuvir (and its predominant circulating metabolite GS-331007). The target enrolment per treatment group was approximately 15 patients. For the PK substudy, intensive serial pharmacokinetic samples were collected (samples obtained over 24 h postdose) at either the week 2 or week 4 treatment visits.

Study assessments

Screening assessments included serum HCV RNA levels and IL28B (rs12979860) genotyping, as well as standard laboratory and clinical tests. Serum HCV RNA was measured with the COBAS® TaqMan® HCV Test, version 2.0, for Use with the High Pure System (Roche Molecular Systems, West Sussex, UK), which has a lower limit of quantification (LLOQ) of 25 IU/mL. HCV genotype and subtype were determined at screening using the Siemens VERSANT HCV Genotype INNO-LiPA 2.0 assay.

On-treatment assessments included standard laboratory testing, serum HCV RNA, vital signs, electrocardiography and symptom-directed physical examinations. All adverse events were recorded and graded according to a standardized scale (see Supplementary Table S7).

NS5B amplification and deep sequencing was performed at DDL Diagnostics Laboratory (Rijswijk, The Netherlands) for all subjects who did not achieve SVR12. Deep sequencing of HCV NS5B was performed at the first virologic failure time point if a plasma/serum sample was available and HCV RNA was >1000 IU/mL, along with the respective baseline samples. Amino acid substitutions in NS5B in the samples collected at virologic failure were compared with the genotype 2 reference and the respective baseline sequence for each patient.

The population pharmacokinetic parameters for sofosbuvir and GS-331007 were computed for all subjects from concentration data from intensive and/or sparse samples using the previously established sofosbuvir and GS-331007 population PK models [11].

Statistical analysis

For treatment-naïve patients without cirrhosis, the SVR12 rate was compared to an adjusted historical SVR rate of 69%, using a two-sided exact one-sample binomial test. The historical control rate was calculated from the weighted average of historical SVR rates for noncirrhotic,

treatment-naïve Japanese patients with genotype 2 HCV infection receiving 24 weeks of Peg-IFNα+RBV (79% with a 10% discount applied due to the expected improvement in safety profile and shorter treatment duration – see Supplementary Table S2 for further details). We calculated that a sample size of 50 patients would provide 80% power to detect an 18% improvement in the SVR12 rate over the adjusted historical rate at a significance level of 0.05. For SVR12 rates for the overall population, for treatment-naïve patients with cirrhosis, and for previously treated patients, statistical hypothesis testing was not performed. For these outcomes, we calculated point estimates of SVR12 rates with two-sided 95% exact confidence interval using the binomial distribution (Clopper–Pearson method).

Study oversight

This trial was approved by the institutional review board or independent ethics committees at all participating sites and was conducted in accordance with local regulations and with recognized international scientific and ethical standards, including the International Conference on Harmonization (ICH) guideline for Good Clinical Practice (GCP) and the original principles embodied in the Declaration of Helsinki. The study was designed and conducted according to protocol by the sponsor (Gilead Sciences) in collaboration with the principal investigators. The sponsor collected the data, monitored study conduct and performed the statistical analyses. The manuscript was prepared by Gilead Sciences with input from all authors.

RESULTS

Baseline characteristics

Of the 188 patients who were initially screened, 153 (90 treatment-naïve and 63 previously treated patients) were enrolled and began treatment (Table S1 and Figure S1). The demographic and baseline clinical characteristics of the patients are provided in Table 1. Overall, the majority of patients were female (54%), and all were Japanese. The mean age was 57 years (ranging from 25 to 74 years) and 22% were aged 65 or older.

Previously treated patients were slightly older than the treatment-naïve patients, with a higher percentage of males, higher baseline viral load, with a higher prevalence of cirrho-

Table 1 Baseline Demographic Characteristics

Characteristic	Overall (N = 153)	Treatment naïve (n = 90)	Previously treated (n = 63)
Mean age, years (range)	57 (25, 74)	55 (25, 73)	60 (34, 74)
Mean BMI, kg/m^2 (range)	24 (16.5, 34)	24 (17, 34)	24 (16.5, 34)
Male, n (%)	70 (46)	33 (37)	37 (59)
Mean HCV RNA, $\log_{10}$ IU/mL ± SD	6.3 (0.84)	6.2 (0.92)	6.5 (0.66)
HCV RNA ≥5 $\log_{10}$ IU/mL, n (%)	140 (92)	78 (87)	62 (98)
HCV genotype, n (%)			
2a	92 (60)	52 (58%)	40 (63%)
2b	61 (40)	38 (42%)	23 (37%)
Cirrhosis, n (%)			
No	136 (89)	82 (91)	54 (86)
Yes	17 (11)	8 (9)	9 (14)
IL28B genotype, n (%)			
CC	121 (79)	73 (81)	48 (76)
CT	28 (18)	17 (19)	11 (17)
TT	4 (3)	0	4 (6)
Median baseline ALT, U/L (range)	34 (12, 412)	32 (12, 412)	36 (12, 232)
Baseline ALT >1.5 × ULN, n (%)	43 (28)	28 (31)	15 (24)
Interferon eligibility, n (%)*			
Interferon eligible	72 (80)	72 (80)	Not applicable
Interferon ineligible	5 (6)	5 (6)	Not applicable
Interferon unwilling	13 (14)	13 (14)	Not applicable
Response to prior HCV treatment, n (%)			
Nonresponse	15 (24)	Not applicable	15 (24)
Relapse/breakthrough	45 (71)	Not applicable	45 (71)
Interferon intolerant	3 (5)	Not applicable	3 (5)
Median eGFR, mL/min (range)	85 (51, 209)	86 (52, 175)	84 (51, 209)

*Interferon eligibility was determined by the site investigator based on whether or not, in their judgment, the patient had contraindications to interferon therapy.

sis and non-CC IL28B genotype. Overall, 11% of participating subjects had cirrhosis. The proportions of patients infected with genotype 2a and 2b HCV were 60% and 40%, respectively, which is similar to previous reports of HCV subtype distribution in the Japanese population [4]. Most (80%) of the treatment-naïve patients were considered eligible for interferon therapy, with 6% having contraindications to interferon therapy and 14% unwilling to receive this treatment. Most (71%) of the previously treated patients had experienced virologic breakthrough or relapse after previous treatment, with 24% reporting nonresponse to prior therapy.

Efficacy

Overall, 148 of the 153 patients (97%, 95% confidence interval [CI] 93–99%) achieved SVR12 (Table 2). By prior treatment history, 88 of the 90 treatment-naïve patients (98%, 95% CI, 92–100%) and 60 of the 63 previously treated patients (95%, 95% CI, 87–99%) achieved SVR12. Of the 82 treatment-naïve patients without cirrhosis, 80 (97%, 95% CI 91–100%) achieved SVR12, thus meeting the primary efficacy endpoint for this group of superiority to the adjusted historical control rate of 69% ($P < 0.001$). Of note, all eight treatment-naïve patients (100%) with cirrhosis and eight of the nine previously treated patients with cirrhosis (89%) achieved SVR12. Overall, 16 of the 17 patients with cirrhosis (94%, 95% CI 71–100%) achieved SVR12.

Patient responses according to baseline characteristics are shown in Supplementary Table S3. Rates of SVR12 were high in all subgroups of patients. Patients with characteristics historically associated with poor response to interferon-based treatment – non-CC IL28B genotype, high baseline viral load, elderly patients, cirrhosis – had rates of SVR12 similar to those in patients without these characteristics.

Relapse accounted for all cases of virologic failure; there were no patients with virologic breakthrough or nonresponse during treatment. Among all patients treated, 97% had HCV RNA <LLOQ by treatment week 2, and 100% achieved HCV RNA <LLOQ by treatment week 4. Overall, five patients experienced virologic relapse after the end of therapy: two (2%) treatment-naïve patients and three (5%) treatment-experienced patients. Four patients relapsed by post-treatment week 4, and one patient relapsed between post-treatment weeks 4 and 12. Characteristics of patients who relapsed are provided in Table S4. There were no consistent host or viral characteristics in the five subjects who relapsed; however, the number of virologic failures is too small for any conclusions to be drawn concerning predictors of virologic failure. No patient relapsed after post-treatment week 12. All 148 SVR12 patients (100%) also achieved SVR24.

Viral resistance testing

The NS5B region was deep sequenced in samples collected from the five relapsers at baseline and at the time of relapse. No S282T variant – known to be associated with reduced susceptibility to sofosbuvir – or any other nucleotide inhibitor resistance-associated variants were detected in any patient at relapse. Phenotypic analysis of the NS5B gene showed no change in susceptibility to either sofosbuvir or ribavirin.

Pharmacokinetics

Population pharmacokinetic analysis was performed to estimate the pharmacokinetics of sofosbuvir and its major circulating nucleoside metabolite, GS-331007. The mean (CV%) of steady-state AUC_{0-24} and C_{max} were 973 (31.2) ng*h/mL and 544 (33.6) ng/mL for sofosbuvir ($N = 45$), respectively, and 10 400 (27.2) ng h/mL and 818 (27.9) ng/mL for GS-331007 ($N = 153$), respectively. Within the Japanese study population, there were no clinically relevant differences in the pharmacokinetics of GS-331007 and sofosbuvir, based on age, sex, BMI, cirrhosis status, prior treatment experience or SVR12 outcome.

Safety

Overall, 73% of patients experienced at least one adverse event; however, the majority of patients experiencing

Table 2 Response during and after Treatment

Response	Overall ($N = 153$)	Treatment naïve ($n = 90$)	Previously treated ($n = 63$)
HCV RNA <LLOQ during treatment, *n* (%)*			
At week 2	148 (97%)	88 (98%)	60 (95%)
At week 4	153 (100%)	90 (100%)	63 (100%)
HCV RNA <LLOQ after end of treatment, *n* (%)			
SVR4	149 (97%)	89 (99%)	60 (95%)
SVR12	148 (97%)	88 (98%)	60 (95%)
95% confidence interval	92.5–99%	92–>99%	87–99%
On-treatment failure	0	0	0
Relapse, *n*/*n* (%)	5 (3%)	2 (2%)	3 (5%)

*LLOQ denotes lower limit of quantification, which is 25 IU/mL. SVR denotes sustained virologic response.

adverse events (84%) had only mild (grade 1) events. The most common treatment-emergent adverse events were nasopharyngitis (upper respiratory viral illness), anaemia, headache, malaise and pruritus (Table 3). No patient in the study discontinued treatment prematurely due to adverse events (or for any other reason). Twenty-two patients (14%) had adverse events that led to modification or interruption of a study drug; 20 patients had ribavirin dose reductions to manage anaemia, and one patient interrupted sofosbuvir and RBV for 1 day because of an event of nasopharyngitis. All but one of the 22 patients with modification or interruption of study drugs achieved SVR12. Two patients experienced treatment-emergent serious adverse events: one treatment-experienced 63-year-old woman had a worsening of anaemia for which she was hospitalized, and one treatment-naïve 36-year-old woman had a severe anaphylactic reaction to a bee sting. No patient experienced a life-threatening (grade 4) adverse event, and only three patients experienced severe (grade 3) events, two of which were deemed to be related to study treatment, the above-mentioned case of anaemia and one case of transient, ribavirin-associated hyperbilirubinaemia in a treatment-experienced 65-year-old man, which resolved during follow-up.

The overall rates of adverse events in younger (<65 years) and older (≥65 years) patients did not differ substantially (72% *vs* 76%, respectively), although there was a higher incidence of anaemia and pruritus in older patients (Table S5). The incidence and severity of adverse events in patients with and without cirrhosis at baseline were similar (Table S6).

Table 3 Discontinuations, Adverse Events and Laboratory Abnormalities by Age

Parameter	Overall (N = 153)
Discontinuation of any study drug due to adverse event	0
Serious adverse events	2 (1%)
Anaemia	1 (1%)
Anaphylactic reaction	1 (1%)
Any adverse event	112 (73%)
Common adverse events*	
Nasopharyngitis	45 (29%)
Anaemia	18 (12%)
Headache	15 (10%)
Malaise	11 (7%)
Pruritus	9 (6%)
Laboratory abnormalities, n (%)	
Decreased haemoglobin concentration	
<10 g/dL	19 (12%)
<8 g/dL	1 (1%)
Neutropenia (500–<750 per mm^3)	1 (1%)
Hyperglycaemia (>250–500 mg/dL)	3 (2%)
Hyperbilirubinaemia (>2.5–5.0 × ULN)	2 (1%)

ULN, upper limit of normal.
*Adverse events occurring in at least 5% of patients.

Overall, the mean change in haemoglobin from baseline to week 12 of treatment was −1.2 g/dL. For patients aged 65 and older, the mean change in haemoglobin was −1.7 g/dL, as compared with 1.0 g/dL in patients under the age of 65. Of all 153 patients enrolled and treated, 19 (12%) had at least one postbaseline haemoglobin value of <10.0 g/dL, and one (1%) had a postbaseline haemoglobin value of <8.5 g/dL. Two patients (1%) had grade 3 hyperbilirubinaemia; no grade 4 hyperbilirubinaemia occurred. One patient, who had grade 2 neutropenia at baseline, had transitory grade 3 neutropenia.

DISCUSSION

In this phase 3 trial, twelve weeks of treatment with sofosbuvir and RBV resulted in high rates of sustained virologic response (>95%) in treatment-naïve and previously treated Japanese patients with chronic genotype 2 HCV infection. Patients with host and viral characteristics that have historically been predictive of lower rates of SVR – older age, presence of cirrhosis, high viral load, non-CC IL28B alleles – had rates of SVR12 similar to patients without these characteristics. In patients who had been previously treated for HCV infection, the nature of the prior response was not associated with significant differences in rates of SVR following treatment with sofosbuvir and ribavirin; patients who had nonresponse to prior treatment had similar response rates as patients who had previously experienced relapse or viral breakthrough. No clear or consistent baseline predictors of treatment failure were evident among the five patients who relapsed after treatment.

The current standard-of-care treatment for Japanese patients with chronic genotype 2 HCV infection is 24 weeks of Peg-IFNα+RBV. Although patients who received this regimen in clinical trials achieved SVR12 rates ranging from 72% to 86%, these studies were restricted to patients <65 years of age [12,13]. However, the Japanese population chronically infected with genotype 2 HCV includes many patients with characteristics that make the use of interferon-based therapy problematic – older age, progressive liver disease, prior treatment experience and comorbid conditions such as diabetes and cardiovascular disease [14]. Moreover, many patients cannot receive interferon therapy due to relative or absolute contraindications. The interferon-free combination of sofosbuvir and ribavirin may represent a promising treatment option for these patients.

Given the characteristics of the patient population in Japan with HCV infection – generally older, and more likely to have advanced liver disease – safety and tolerability of therapeutic regimens is an important issue. In the present study, 22% of patients were aged 65 or older and 11% had cirrhosis. Analyses of safety data by age (<65 *vs*

≥65 years) showed increases in reported adverse events and laboratory abnormalities in older patients, but these differences did not present a barrier to treatment as no premature discontinuation of study treatment occurred in any patient. Analysis of safety data according to the presence or absence of cirrhosis did not indicate clinically important differences in safety or tolerability of the 12-week sofosbuvir plus ribavirin regimen.

Consistent with previous reports, the results of this study confirm the high barrier to resistance afforded by the sofosbuvir plus RBV treatment regimen. Rapid viral suppression was observed with all patients achieving HCV RNA undetectable status by week 4, with no virologic breakthrough observed during treatment in any of the 153 patients. The percentage of patients who relapsed after treatment was low (3%), and none of the subjects who relapsed had S282T or other nucleoside inhibitor resistance-associated variants. No change in susceptibility to sofosbuvir or ribavirin compared with the corresponding baseline or wild-type reference was observed at the relapse time point.

The main limitation of this study was the lack of a control arm to allow direct comparison with interferon-based regimens. Several considerations guided our choice of an uncontrolled study design. Adding an interferon-based control arm would have required exclusion of patients who were ineligible to receive or intolerant of interferon – an important and substantial proportion of patients – as well as previously treated patients, for whom further interferon treatment is not an option. Moreover, given that Peg-IFNα is administered by subcutaneous injection, blinding of treatment arms would not have been possible.

In conclusion, treatment with the all-oral, interferon-free combination of sofosbuvir and RBV resulted in high rates of sustained virologic response in both treatment-naïve and previously treated Japanese patients with chronic genotype 2 HCV infection. The degree of antiviral efficacy coupled with a favourable safety and tolerability profile, including patients with cirrhosis and those aged 65 and older, suggest that this combination may fill an important unmet medical need in Japan.

ACKNOWLEDGMENTS AND DISCLOSURES

Supported by Gilead Sciences. We thank the patients and their families, as well as the investigators and site personnel. In addition, we thank Juan Betular, Camilla Lau and Ellen Milner of Gilead Sciences for their contributions to study conduct. Writing assistance was provided by David McNeel of Gilead Sciences.

REFERENCES

1 Chung H, Ueda T, Kudo M. Changing trends in hepatitis C infection over the past 50 years in Japan. *Intervirology* 2010; 53: 39–43.
2 Tanaka J, Kumgai J, Katayama K *et al.* Sex- and age-specific carriers of hepatitis B and C viruses in Japan estimated by the prevalence in the 3,485,648 first-time blood donors during 1995–2000. *Intervirology* 2004; 47: 32–40.
3 Mizokami M, Tanka Y, Miyakawa Y. Spread times of hepatitis C virus estimated by the molecular clock differ among Japan, the United States and Egypt in reflection of their distinct socioeconomic backgrounds. *Intervirology* 2006; 49: 28–36.
4 Thein HH, Yi Q, Dore GJ, Krahn MD. Estimation of stage-specific fibrosis progression rates in chronic hepatitis C virus infection: a meta-analysis and metaregression. *Hepatology* 2008; 48: 418–431.
5 Toyoda H, Kumada T, Takaguchi K, Shimada N, Tanaka J. Changes in hepatitis C virus genotype distribution in Japan. *Epidemiol Infect* 2014.
6 Kumada H, Okanoue T, Onji M *et al.* Guidelines for the treatment of chronic hepatitis and cirrhosis due to hepatitis C virus infection for the fiscal year 2008 in Japan. *Hepatol Res* 2010; 40: 8–13.
7 Sovaldi (sofosbuvir) Tablets: US Prescribing Information. Foster City, CA: Gilead Sciences, December 2013. Available at: http://www.gilead.com/~/media/Files/pdfs/medicines/liver-disease/sovaldi/sovaldi_pi.pdf.
8 Lawitz E, Mangia S, Wyles D *et al.* Sofosbuvir for previously untreated chronic hepatitis C infection. *N Engl J Med* 2013; 368: 1878–1887.
9 Jacobson IM, Gordon SC, Kowdley KV *et al.* Sofosbuvir for hepatitis C genotype 2 or 3 in patients without treatment options. *N Engl J Med* 2013; 368: 1867–1877.
10 Zeuzem S, Dusheiko GM, Salupere R *et al.* Sofosbuvir and ribavirin in HCV genotypes 2 and 3. *N Engl J Med* 2014; 370: 1993–2001.
11 Kirby B, Gordi T, Symonds WT, Kearney BP, Mathias A. Population pharmacokinetics of sofosbuvir and its major metabolite (GS-331007) in healthy and HCV-infected adult subjects. AASLD Annual Meeting 2013.
12 Kanda T, Imazeki F, Azemoto R *et al.* Response to peginterferon-alfa 2b and ribavirin in Japanese patients with chronic hepatitis C genotype 2. *Dig Dis Sci* 2011; 56: 3335–3342.
13 Inoue Y, Hiramatsu N, Oze T *et al.* Factors affecting efficacy in patients with genotype 2 chronic hepatitis C treated by pegylated interferon alpha-2b and ribavirin: reducing drug doses has no impact on rapid and sustained virological responses. *J Viral Hepat* 2010; 17: 336–344.
14 Asahina Y, Tsuchiya K, Tamaki N *et al.* Effect of aging on risk for hepatocellular carcinoma in chronic hepatitis C virus infection. *Hepatology* 2010; 52: 518–527.

SUPPORTING INFORMATION

Additional Supporting Information may be found in the online version of this article:

Fig. S1. Patient disposition.

Table S1. Reasons for screen failure.

Table S2. Calculation of the adjusted historical control rate.

Table S3. SVR12 by subgroup.

Table S4. Characteristics of patients who relapsed.

Table S5. Common adverse events by age group.

Table S6. Common adverse events by cirrhosis status.

Table S7. Gilead sciences grading scale for severity of adverse events and laboratory abnormalities.

Carcinogenesis vol.35 no.2 pp.272–281, 2014
doi:10.1093/carcin/bgt343
Advance Access publication October 15, 2013

Heat shock factor 1 accelerates hepatocellular carcinoma development by activating nuclear factor-κB/mitogen-activated protein kinase

Makoto Chuma*, Naoya Sakamoto, Akira Nakai[1], Shuhei Hige, Mitsuru Nakanishi, Mitsuteru Natsuizaka, Goki Suda, Takuya Sho, Kanako Hatanaka[2], Yoshihiro Matsuno[2], Hideki Yokoo[3], Toshiya Kamiyama[3], Akinobu Taketomi[3], Gen Fujii[4], Kosuke Tashiro[5], Yoko Hikiba[6], Mitsuaki Fujimoto[1], Masahiro Asaka and Shin Maeda[7]

Department of Gastroenterology and Hepatology, Hokkaido University, Kita 15, Nishi 7, Kita-ku, Sapporo 060-8638, Japan, [1]Department of Biochemistry and Molecular Biology, Yamaguchi University, Ube, Japan, [2]Department of Pathology and [3]Department of Gastroenterological Surgery I, Hokkaido University, Kita 15, Nishi 7, Kita-ku, Sapporo 060-8638, Japan, [4]Division of Cancer Prevention, National Cancer Center Research Institute, Tokyo, Japan, [5]Graduate School of Genetic Resources Technology, Kyushu University, Fukuoka, Japan, [6]Division of Gastroenterology, Institute for Adult Diseases, Asahi Life Foundation, Tokyo, Japan and [7]Department of Gastroenterology, Yokohama City University, Yokohama, Japan

*To whom correspondence should be addressed. Tel: +81 11-716-1611; Fax: +81 11-706-7867;
Email: mchuuma@med.hokudai.ac.jp

Heat shock factor 1 (HSF1), a major transactivator of stress responses, has been implicated in carcinogenesis in various organs. However, little is known about the biological functions of HSF1 in the development of hepatocellular carcinoma (HCC). To clarify the functional role of HSF1 in HCC, we established HSF1-knockdown (HSF1 KD) KYN2 HCC cells by stably expressing either small hairpin RNA (shRNA) against HSF1 (i.e. HSF1 KD) or control shRNA (HSF1 control). Tumorigenicity was significantly reduced in orthotopic mice with HSF1 KD cells compared with those with HSF1 control cells. Reduced tumorigenesis in HSF1 KD cells appeared attributable to increased apoptosis and decreased proliferation. Tumor necrosis factor-α-induced apoptosis was increased in HSF1 KD cells and HSF1$^{-/-}$ mouse hepatocytes compared with controls. Decreased expression of IκB kinase γ, a positive regulator of nuclear factor-κB, was also observed in HSF1 KD cells and HSF1$^{-/-}$ mouse hepatocytes. Furthermore, expression of bcl-2-associated athanogene domain 3 (BAG3) was dramatically reduced in HSF1 KD cells and HSF1$^{-/-}$ mouse hepatocytes. We also found that epidermal growth factor-stimulated mitogen-activated protein kinase signaling was impaired in HSF1 KD cells. Clinicopathological analysis demonstrated frequent overexpression of HSF1 in human HCCs. Significant correlations between HSF1 and BAG3 protein levels and prognosis were also observed. In summary, these results identify a mechanistic link between HSF1 and liver tumorigenesis and may provide as a potential molecular target for the development of anti-HCC therapies.

Introduction

Hepatocellular carcinoma (HCC) is one of the most common malignant tumors and the third leading cause of cancer death worldwide (1). Despite marked advances in diagnostic and therapeutic techniques, prognosis remains unsatisfactory for HCC patients (2,3). An understanding of HCC carcinogenesis at the molecular level is thus urgently needed in order to identify novel molecular targets for the development of more effective therapies.

Heat shock factor 1 (HSF1) is the main regulator of the heat shock response, which is involved in protecting cells and organisms from heat, ischemia, inflammation, oxidative stress and other noxious conditions (4,5). Under various forms of physiological stress, HSF1 drives the production of heat shock proteins (HSPs), such as HSP27, HSP70 and HSP90, which act as protein chaperones (5,6). The functions of HSF1 are not limited to increasing the expression of chaperones; HSF1 also modulates the expression of hundreds of genes other than chaperones that are critical for survival under an array of potentially lethal stressors (6–8). As a result, HSF1 influences fundamental cellular processes such as cell cycle control, protein translation, glucose metabolism and proliferation (7–12). In human tumors, constitutive expression of Hsp27, Hsp70 and Hsp90 at high levels predicts poor prognosis and resistance to therapy (13–15). These effects are often attributable to HSF1-dependent mechanisms (16). Thus, as a master regulator of cellular processes, the roles of HSF1 in carcinogenesis and tumor progression are now emerging. Several recent investigations using mouse models have suggested that HSF1 is involved in carcinogenesis (9,17). In clinical samples, HSF1 is often constitutively expressed at high levels in a variety of tumors, including breast cancer (7,18), pancreatic cancer (19), prostate carcinoma (20) and oral squamous cell carcinoma (21).

Hepatocarcinogenesis is a multistep process, in the majority of cases slowly developing within a well-defined etiology of viral infection and chronic alcohol abuse, leading to the chronic hepatitis and cirrhosis that are regarded as preneoplastic stages (22). A great number of factors, receptors and downstream elements of signaling cascades regulate proliferation and apoptosis. Dysregulation of the balance between cell proliferation and apoptosis thus plays a critical role in hepatocarcinogenesis (23,24). Two of the major pathways of cell proliferation and apoptosis are nuclear factor kappa B (NF-κB) signaling and mitogen-activated protein kinase (MAPK) signaling. NF-κB transcription factors are critical regulators of genes involved in inflammation and the suppression of apoptosis. NF-κB has been shown to be instrumental for tumor promotion in colitis-associated cancer and inflammation-associated liver cancer (25,26). Activation of the extracellular signal-regulated kinase (ERK)/MAPK pathway regulates many important cellular processes, such as proliferation, differentiation, angiogenesis, survival and cell adhesion (27). Importantly, the ERK/MAPK pathway is constitutively activated in HCC (28).

The present study investigated the biological influences of HSF1 in HCC cell proliferation and apoptosis involving the NF-κB and MAPK signal pathways. We found that HSF1 deficiency significantly diminished NF-κB and MAPK activation in primary hepatocytes and HCC cells, so HSF1 deficiency inhibited the development of HCC. Furthermore, clinicopathological analysis demonstrated a significant correlation between HSF1 protein level and prognosis. Our results suggest HSF1 as a promising molecular target for the development of anti-HCC therapeutics.

Abbreviations: BAG3, bcl-2-associated athanogene domain 3; EGFR, epidermal growth factor receptor; ERK, extracellular signal-regulated kinase; FACS, fluorescence-activated cell sorting; HCC, hepatocellular carcinoma; HSF1, heat shock factor 1; HSF1 KD, HSF1 knockdown; HSP, heat shock protein; IKKγ, IκB kinase gamma; LPS, lipopolysaccharide; MAPK, mitogen-activated protein kinase; MEK, mitogen-activated protein kinase kinase; mRNA, messenger RNA; NF-κB, nuclear factor kappa B; PCNA, proliferating cell nuclear antigen; SCID, severe combined immune-deficient mice; shRNA, small hairpin RNA; TNF-α, tumor necrosis factor alpha; TUNEL, terminal deoxynucleotidyl transferase-mediated deoxyuridine triphosphate nick-end labeling; WT, wild type.

Materials and methods

Cell cultures and reagents

Human HCC cell lines HepG2, PLC/PRF/5, HLE and HLF were obtained from the American Type Culture Collection. Huh7 was obtained from the Japanese Collection of Research Bioresources Cell Bank (Ibaraki, Japan). KIM-1 and KYN2 were kindly provided by Dr Hirohisa Yano (Department of Pathology, Kurume University, Kurume, Japan). Li7 was kindly provided by Dr Yae Kanai (Division of Molecular Pathology, National Cancer Center Research Institute,

Tokyo, Japan). HepG2, PLC/PRF/5, Huh7, HLE and HLF cells were maintained in Dulbecco's modified Eagle's medium containing 10% fetal bovine serum. KIM-1 and KYN2 was maintained in RPMI medium containing 10% fetal bovine serum.

Antibodies and chemicals

The antibodies used included: anti-HSF1, ERK1/2, phosphor-ERK1/2, MAPK kinase (MEK), phospho-MEK, phosphor- efficiently activated epidermal growth factor receptor (EGFR), cyclin D1, cdc2, CDK4, phospho-IκBα, IκB kinase gamma (IKKγ), IKKβ, caspase-3 and Bcl-X_L (Cell Signaling Biotechnology, Danvers, MA); anti-HSP90, HSP72, β-actin and proliferating cell nuclear antigen (PCNA) (Santa Cruz Biotechnology, Santa Cruz, CA); anti-EGFR (Millipore, Billerica, MA); anti-HSP70/HSP72 (Enzo Life science, NY); and anti-BAG3 (Abcam, Cambridge, UK).

Biochemical and immunohistochemical analyses

Protein lysates were prepared from tissues and cultured cells, separated by sodium dodecyl sulfate–polyacrylamide gel electrophoresis, transferred onto Immobilon membranes (Millipore) and analyzed by immunoblotting. Total cellular RNA was extracted using Trizol reagent (Invitrogen, Carlsbad, CA), then cDNA was synthesized using SuperScript II (Invitrogen), and expression of specific messenger RNAs (mRNAs) was quantified using real-time PCR and normalized against glyceraldehyde-3-phosphate dehydrogenase mRNA expression. Details of real-time PCR conditions and primer sequences are available in Supplementary Materials and methods, available at *Carcinogenesis* Online. Immunohistochemical staining was performed on formalin-fixed, paraffin-embedded tissue sections using immunoperoxidase methods, as described previously (15). For array analysis, we used the Human WG-6 BeadChip-kit (Illumina, San Diego, CA) in accordance with the instructions from the manufacturer (details are given in Supplementary Materials and methods, available at *Carcinogenesis* Online).

Establishment of HSF1-knockdown cells

A HSF1 small hairpin RNA (shRNA) plasmid and negative control plasmid were purchased from SABiosciences (QIAGEN, Valencia, CA). The shRNA sequences targeting HSF1 were from position 5′-CAGGTTGTTCATAGTCAGAAT-3′ as in the nucleotide sequence of HSF1. As a negative control, a shRNA was designed with the sequence 5′-GGAATCTCATTCGATGCATAC-3′. Transfection was achieved using Oligofectamine reagent (Invitrogen) according to the instructions from the manufacturer. To establish stable knockdown cell lines, shRNA plasmids were transfected into KYN2 cells and cultured in the presence of puromycin (Sigma–Aldrich, St Louis, MO).

Cell proliferation and bromodeoxyuridine assay

Cell proliferation in response to HSF1 silencing was determined by trypan blue exclusion assay. DNA synthesis was determined by bromodeoxyuridine assay according to the instructions from the manufacturer (Roche Diagnostics, Basel, Switzerland). The result was expressed as a percentage of the maximum absorbance at 450nm, based on three independent experiments. Cells were counted using a Coulter Counter (Beckman Coulter, Pasadena, CA).

Apoptosis assay

Assessment of apoptosis was performed by measuring the intensity of the sub-G_1 peak. For the sub-G_1 peak, HSF1 control KYN2 cells or HSF1-knockdown (HSF1 KD) KYN2 cells were tumor necrosis factor alpha (TNF-α) treatment for 24 h. Cells were treated with propidium iodide and then the sub-G_1 peak was analyzed with a fluorescence-activated cell sorting (FACS) flow cytometer (FACSCalibur; Becton Dickinson, San Jose, CA). Terminal deoxynucleotidyl transferase-mediated deoxyuridine triphosphate nick-end labeling (TUNEL) assay was performed in accordance with the manufacturer's instructions (ApopTag kit; Intergen, Burlington, MA).

Animals

HSF1-deficient ($HSF^{-/-}$) mice have been described previously (29). C57BL/6 wild-type (WT) mice were purchased from CLEA Japan (Tokyo, Japan) for use in the experiments, with primary hepatocytes isolated using a collagenase perfusion method as described in a previous report (26). For orthotopic implantation, C.B-17/Icr-scid/scidJcl [severe combined immune-deficient mice (SCID)] mice were obtained from CLEA Japan. All mice were maintained in filter-topped cages on autoclaved food and water at the University of Hokkaido and the Institute for Adult Diseases, Asahi Life Foundation, according to National Institutes of Health (NIH) guidelines. All experimental protocols were approved by the ethics committee for animal experimentation at Hokkaido University and Asahi Life Foundation. Orthotopic implantation of KYN2 cells and KYN2 transfectants were performed as described previously (30). Briefly, mice were inoculated orthotopically with 5×10^6 HSF1 control ($n = 12$) and HSF1 KD ($n = 12$) cells in 100 µl of phosphate-buffered saline, injected into the liver. Mice were killed 6 weeks after inoculation and autopsies were performed immediately. In the lipopolysaccharide (LPS)/D-galactosamine (GalN)-induced liver injury model, mice were injected intraperitoneally with LPS (20 lg/kg; Sigma) and GalN (1000 mg/kg; Wako, Osaka, Japan) (24).

Patients and tissue samples

For immunohistochemical analysis, a total of 226 adult patients with HCC who underwent curative resection between 1997 and 2006 at Hokkaido University Hospital were enrolled in this study. A preoperative clinical diagnosis of HCC was required to meet the diagnostic criteria of the American Association for the Study of Liver Diseases. Briefly, inclusion criteria were as follows: (i) distinctive pathological diagnosis, (ii) no preoperative anticancer treatment or distant metastases, (iii) curative liver resection (exclusion of extrahepatic tumor spread/metastasis) and (iv) complete clinicopathological and follow-up data. The study protocols were approved by the institutional review board and performed in compliance with the Helsinki of Declaration. Written informed consent was obtained from as many of the patients who were alive as possible (deceased cases were approved for use without written informed consent). Histological diagnosis was made according to World Health Organization criteria. The main clinicopathological features are presented in Table I. During follow-up, clinical evaluations and biochemical tests were performed every 1–3 months. Patients underwent triphasic computed tomography of the liver every 2–3 months.

Statistical analysis

Data are expressed as mean ± standard error of the mean (SEM). Significant differences were detected using non-parametric testing. Correlations between protein expression and clinicopathological features of the specimens were assessed, and the resulting data were analyzed using the χ^2 test and Fisher's exact test. Cumulative survival rate was calculated from the first date of treatment using the Kaplan–Meier life-table method. Differences were evaluated by log-rank testing. Independent factors for survival were assessed with the Cox proportional hazard regression model. Differences between the two groups were analyzed using the log-rank test. Statistical analyses were performed using Stat View software (version 5.0; SAS Institute, Cary, NC). Values of $P < 0.05$ were considered significant.

Results

Effect of HSF1 on tumor growth

We first investigated expression of HSF1 in cultured HCC cell lines. HSF1 expression was detected in all eight HCC cell lines analyzed. KYN2 cells showed significantly higher expression of HSF1 than other cell lines (Figure 1A). To further elucidate the functional role of HSF1 in HCC, we established HSF1 KD KYN2 cells by expressing the shRNA against HSF1 or control shRNA. To evaluate the effects of HSF1 on cell growth, we measured cell numbers at several time points and found that the growth of HSF1 KD cells was significantly inhibited compared with control cells (HSF1 control) (Figure 1B). Cell cycle regulators including PCNA, cyclin D1, cdc2 and CDK4 were suppressed in HSF1 KD cells compared with HSF1 control cells (Figure 1C). These results indicate that HSF1 enhances HCC cell growth. Concordantly, HSF1 KD reduced DNA synthesis as measured by bromodeoxyuridine incorporation (Figure 1D).

To evaluate the effects of HSF1 on HCC *in vivo*, orthotopic xenografts were established by HSF1 control and HSF1 KD KYN2 cells in nude mice. Maximum primary tumor diameters and tumor volumes were significantly decreased in HSF1 KD xenografts compared with HSF1 control ones (Figure 1E), suggesting that HSF1 accelerated HCC tumor growth *in vivo*. We confirmed that the tumor of HSF1 KD cells showed significantly lower expression of HSF1 and PCNA than the tumor of HSF1 control cells (Figure 1E).

We performed gain-of-function experiments for HSF1 *in vitro*. No apparent changes in cell growth were seen with overexpression of HSF1 in HCC cell lines with low HSF1 expression (Supplementary Figure 1, available at *Carcinogenesis* Online), whereas cell growth was reduced in HSF1 KD experiments, as above. Based on these